JAMES | Journal of Advances in Modeling Earth Systems

RESEARCH ARTICLE
10.1029/2023MS003924

Special Collection:
Using radiative-convective equilibrium to understand convective organization, clouds, and tropical climate

How Does Organized Convection Impact Explicitly Resolved Cloud Feedbacks in the Radiative-Convective Equilibrium Model Intercomparison Project?

Catherine L. Stauffer[1] and **Allison A. Wing**[1]

[1]Department of Earth, Ocean and Atmospheric Science, Florida State University, Tallahassee, FL, USA

Key Points:

- Domains with organized convection have cloud feedbacks with the same sign but larger inter-model spread than domains without organization
- The cloud feedback parameter is less positive, or even negative, for more strongly organized domains
- In radiative-convective equilibrium, the tropical anvil cloud area feedback is positive due to the shortwave cloud optical depth feedback

Supporting Information:

Supporting Information may be found in the online version of this article.

Correspondence to:

C. L. Stauffer,
catherine.stauffer@mcgill.ca

Citation:

Stauffer, C. L., & Wing, A. A. (2024). How does organized convection impact explicitly resolved cloud feedbacks in the radiative-convective equilibrium model intercomparison project? *Journal of Advances in Modeling Earth Systems*, *16*, e2023MS003924. https://doi.org/10.1029/2023MS003924

Received 14 JUL 2023
Accepted 15 AUG 2024

Abstract In simulations of radiative-convective equilibrium (RCE), and with sufficiently large domains, organized convection enhances top of atmosphere outgoing longwave radiation due to the reduced cloud coverage and drying of the mean climate state. As a consequence, estimates of climate sensitivity and cloud feedbacks may be affected. Here, we use a multi-model ensemble configured in RCE to study the dependence of explicitly calculated cloud feedbacks on the existence of organized convection, the degree to which convection within a domain organizes, and the change in organized convection with warming sea surface temperature. We find that, when RCE simulations with organized convection are compared to RCE simulations without organized convection, the propensity for convection to organize in RCE causes cloud feedbacks to have larger magnitudes due to the inclusion of low clouds, accompanied by a much larger inter-model spread. While we find no dependence of the cloud feedback on changes in organization with warming, models that are, on average, more organized have less positive, or even negative, cloud feedbacks. This is primarily due to changes in cloud optical depth in the shortwave, specifically high clouds thickening with warming in strongly organized domains. The shortwave cloud optical depth feedback also plays an important role in causing the tropical anvil cloud area feedback to be positive which is directly opposed to the expected negative or near zero cloud feedback found in prior work.

Plain Language Summary Tropical clouds play an important role in the uncertainty associated with understanding how the Earth's climate responds to an imposed warming. Here, we look at how organized cloud systems associated with the tropics affect the processes that govern the climate response to warming. We find that strongly organized cloud systems reduce how strongly the Earth responds to warming. This is primarily associated with the changes in the optical properties of high clouds. These cloud properties impact the overall understanding of the role tropical clouds play in modulating the Earth's temperature and calls into question prior assumptions of its behavior.

1. Introduction

Understanding estimates in equilibrium climate sensitivity, which is the global mean surface temperature response to a doubling of CO_2, is a key component in understanding the impacts of climate change on society. Despite increasingly sophisticated models, there has been relatively little advancement in reducing the uncertainty in estimates of climate sensitivity, until recently (Knutti et al., 2017; Sherwood et al., 2020; Zelinka et al., 2020). However, *understanding* of estimates of climate sensitivity, climate feedbacks, and the uncertainties associated with them have had significant advancements (Sherwood et al., 2020; Zelinka et al., 2020). In an effort to narrow the focus of research in climate science, Bony et al. (2015) proposed a series of questions that are in need of being addressed, accompanied by a grand challenge for research in model development, observational campaigns, and physical understanding to be tailored toward these questions. Two of these questions concerned the role convection plays in cloud feedbacks and the role organized convection plays in climate sensitivity. This is because cloud feedbacks, and tropical cloud feedbacks in particular, are continually the largest source of uncertainty in the climate feedback parameter and, subsequently, estimates of climate sensitivity (Dufresne & Bony, 2008; Sherwood et al., 2014; Soden & Held, 2006; Soden & Vecchi, 2011; Vial et al., 2013; Zelinka et al., 2013).

Similar uncertainties in the cloud feedbacks were found using a combination of multiple lines of evidence, including observations, paleoclimate records, and high-resolution process modeling (Sherwood et al., 2020). A problem in addressing these issues involves the need for global climate models to parameterize convection,

thereby neglecting key physical processes (Li et al., 2012; Waliser et al., 2009). In this study, we will address this problem by returning to a simplified configuration of the atmosphere to consider cloud feedbacks in an ensemble of models that explicitly represent convection. The simplification used here is an idealized framework ideally suited to studying tropical deep convection called radiative-convective equilibrium (RCE), which is a statistical balance between radiative cooling and convective heating (Jakob et al., 2019; Tompkins & Craig, 1998). Model hierarchies consist of increasingly complex systems that can connect understandings of complex climate processes through simpler settings (Held, 2005). RCE is a critical part of such a model hierarchy through its elimination of large-scale dynamical instabilities due to heterogeneous boundary conditions or forcing (Jeevanjee et al., 2017; Maher & Gerber, 2019). RCE simulations support a range of spatial resolutions and model types (Becker & Wing, 2020; Cronin & Wing, 2017; Tompkins & Craig, 1998; Wing et al., 2020a), a feature that is exploited by the Radiative-Convective Equilibrium Model Intercomparison Project (RCEMIP; Wing et al., 2018, 2020a). The collection of models contained within RCEMIP includes cloud resolving models (CRMs), which explicitly resolve convection, as well as general circulation models (GCMs), which parameterize convection.

Cloud feedback estimates in highly-idealized simulations of RCE have typically been limited to approximations using the changes in cloudy-sky top of atmosphere radiative fluxes (known as the cloud radiative effect, or CRE) or by analyzing the processes that cause high clouds to change with warming (Ohno & Satoh, 2018; Ohno et al., 2019, 2020, 2021). However, these metrics do not provide a complete explanation of the cloud impacts on the climate (Cess & Potter, 1988). To the best of our knowledge, only two studies have used CRMs configured in RCE to calculate cloud feedbacks by explicitly accounting for the changes in various cloud and atmospheric properties. Cronin and Wing (2017) used a kernel-correction approach to compute cloud feedbacks in one CRM. Radiative kernels better characterize radiative feedbacks and allow for a cleaner comparison to GCMs, but still have limits in the understanding of certain processes governing the feedbacks. Using the CRMs in RCEMIP, Stauffer and Wing (2023) recently explicitly computed cloud feedbacks and decomposed said cloud feedbacks into contributions due to changes in cloud amount, cloud altitude, and cloud optical depth following the cloud radiative kernel (CRK) method of Zelinka et al. (2013). They found that, despite only representing tropical deep-convecting clouds, RCE does remarkably well at capturing the global cloud feedback (such as those by GCMs, Zelinka et al., 2020).

The cloud feedbacks in RCEMIP computed by Stauffer and Wing (2023), however, were limited to the simulations of the "RCE_small" domain, where few low clouds were produced and for which the domain was not sufficiently large for convection to self-aggregate. Convective self-aggregation is a phenomenon that emerges in RCE and is defined as the spontaneous organization of convection despite homogeneous boundary conditions and forcing, whose presence influences many climate variables (Wing et al., 2017). Generally, convective self-aggregation reduces the domain-mean extent of high clouds, dries the mean state, and allows for more efficient radiative cooling to space (i.e., an increase in outgoing longwave radiation, or OLR, associated with the drying of the mean state, Wing, 2019; Wing et al., 2017). These responses are found in both idealized model simulations (e.g., Bony et al., 2016; Wing & Cronin, 2016; Wing & Emanuel, 2014; Wing et al., 2020a) and in observations of aggregated convection and monthly variations in aggregation over the entire tropics (e.g., Bony et al., 2020; Tobin et al., 2012, 2013). Convective self-aggregation, and the associated drying of the mean climate state and decreased high cloud coverage, may affect climate sensitivity where high levels of convective self-aggregation (or increases in aggregation with warming) might reduce the climate sensitivity (Becker & Stevens, 2014; Becker et al., 2017; Bony et al., 2015; Coppin & Bony, 2018; Cronin & Wing, 2017; Hohenegger & Stevens, 2016; Mauritsen & Stevens, 2015).

For the majority of models in RCEMIP, a certain level of organized convection occurs, but with intensities that vary across the models and which have an inconsistent change with warming sea surface temperature (SST; Wing et al., 2020a). The plethora of models in RCE containing convective self-aggregation in RCEMIP provides ample opportunity to learn about tropical deep convection and how it affects climate sensitivity and cloud feedbacks, as encouraged by the questions posed in Bony et al. (2015). Becker and Wing (2020) found that the extreme spread in the net climate feedback parameter in RCEMIP could be explained by a combination of changes in shallow cloud fraction and convective self-aggregation with warming. As convection becomes more aggregated, enhanced mid-tropospheric drying increases the clear-sky OLR. They based their attribution of aggregation impacts to clear-sky processes based on the fact that the change in aggregation with warming was not correlated with the change in CRE with warming, while it was with the clear-sky climate feedback parameter. However, as discussed above, this may not be a complete view of how aggregation affects cloud feedbacks.

Using an explicit calculation and decomposition of the cloud feedback in RCEMIP, we will look at three ways in which convective self-aggregation can influence cloud feedbacks: (a) the mere existence of organized convection as analyzed by comparing the cloud feedbacks of unaggregated RCE_small simulations to aggregated RCE_large simulations, (b) the variability in the degree to which a domain has organized convection by comparing the cloud feedbacks across the RCE_large models, and (c) the changes in aggregation with warming, also through comparing the cloud feedbacks across the RCE_large ensemble. Here, the term cloud feedback refers to the cloud feedback parameter which is defined as the change in top of atmosphere radiative fluxes per unit of surface temperature change due to changes in clouds. RCEMIP and the cloud feedback computation is described in Section 2, Section 3 describes the cloud feedbacks found in RCE_large while Section 4 discusses how the *degree* to which a domain organizes affects the cloud feedbacks. Section 5 compares the cloud feedbacks in RCE to those in more complex models before closing with a discussion in Section 6.

2. Data and Methods

2.1. RCE Simulations

In this study, we examine the impact of convective organization on cloud feedbacks using the RCEMIP data set (Wing et al., 2018, 2020a). The cloud feedback computation (Sections 2.2 and 2.3) requires six-hourly instantaneous 3D snapshots of temperature, pressure, water vapor (specific humidity), cloud liquid water, and cloud ice water. Calculations of column relative humidity (CRH) also make use of instantaneous 3D snapshots of specific humidity. All data fields are from the last ∼25 days (of ∼100 days) of the simulations and are temporally averaged from this range. We limit the models used to those with explicitly resolved convection because, in addition to data availability, the resolution of the GCMs (∼1° × 1°) is too coarse to resolve clouds and requires an assumption of the sub-grid scale distribution of clouds, which does not have an offline capability, and the grid box-averaged cloud water content is not suitable to use in this study.

To study changing climate in RCE, there are three simulations at three different SSTs: 295, 300, and 305 K; this work will primarily focus on the cloud feedbacks associated with the change from 295 to 305 K. For the models with explicit convection, there are two different domain sizes to study the effects of organized convection on the climate. "RCE_small" simulations do not permit convective self-aggregation to occur and are ∼100 × 100 km^2 with 1 km horizontal resolution and ∼74 vertical levels. "RCE_large" simulations do permit organized convection to occur and are ∼6,000 × 400 km^2 with 3 km horizontal resolution and ∼74 vertical levels. They are initialized from a profile that is temporally- and domain-averaged from the RCE_small simulations. Stauffer and Wing (2023) examined cloud feedbacks in the RCE_small simulations, here we examine RCE_large. The CAM5-GCM and CAM6-GCM simulations from the RCEMIP archive were also re-run to produce the satellite simulator histograms used in the cloud feedback calculation (Reed et al., 2021). This allows for a limited comparison between the CRMs and a model with parameterized convection. These versions of the CAM5-GCM and CAM6-GCM simulations are referred to as CAM5-GCM-RCE and CAM6-GCM-RCE, respectively.

More details on the RCEMIP simulations can be found in the protocol and overview papers (Wing et al., 2018, 2020a).

2.2. ISCCP Histograms

We use the International Satellite Cloud Climatology Project (ISCCP) simulator configured for use with offline data (Stauffer & Wing, 2023, and references therein) to create a joint histogram that describes the distribution of clouds categorized by cloud top pressure (CTP) and cloud optical depth (τ). The ISCCP simulator was designed to compare model data with satellite observations by using the same retrieval techniques employed by remote sensors, and is particularly well suited to cloud feedback applications because it retrieves CTP based on infrared emission temperature (Klein & Jakob, 1999; Rossow & Schiffer, 1991; Webb et al., 2001). The ISCCP simulator was specifically chosen as it was used in the development of the cloud feedback decomposition used in this study (Zelinka et al., 2012a, 2012b). This cloud histogram, in combination with a CRK describing the sensitivity of top of atmosphere radiative fluxes to a 100% increase in clouds partitioned in the same manner as the cloud histogram, allows us to compute cloud feedbacks based on specific changes in CTP and τ.

Table 1
Given Names and Column Relative Humidity (CRH) Ranges in the CRH Bins

Bin name	CRH range	Bin name	CRH range
B010	0% < CRH ≤ 10%	B060	50% < CRH ≤ 60%
B020	10% < CRH ≤ 20%	B070	60% < CRH ≤ 70%
B030	20% < CRH ≤ 30%	B080	70% < CRH ≤ 80%
B040	30% < CRH ≤ 40%	B090	80% < CRH ≤ 90%
B050	40% < CRH ≤ 50%	B100	90% < CRH ≤ 100%

Cloud ice and cloud liquid optical depths were calculated from ice and liquid condensate following the parameterizations of Fu (1996) and Slingo (1989), respectively, as described by Stauffer and Wing (2023). Cloud top pressure is the pressure associated with the temperature that is closest to the infrared brightness temperature corresponding to cloud top temperature, accounting for partial emissivity through clouds. The Cloud Feedback Model Intercomparison Project (CFMIP) Observation Simulator Package (COSP) uses model output to simulate retrievals from several different sensors, such as the often-used ISCCP simulator (Swales et al., 2018). The main difference between the ISCCP simulator used in COSP and the offline simulator is that the latter neglects clear-sky brightness temperature effects (for more details see Stauffer & Wing, 2023).

To consider what the cloud feedback is in the different regimes represented in the RCE_large domain, the domain is sorted into 10 CRH bins that increase in 10% increments from 0%–10% to 90%–100%, the naming convention used throughout this paper is provided in Table 1. CRH is the ratio of mass weighted vertical integrals of specific humidity and saturation specific humidity (Wing et al., 2018, 2020a). We use this as our moisture variable to best capture the troposphere-depth moisture and because of its use in characterizing organized convection in RCEMIP (Wing et al., 2020a). An individual ISCCP histogram and CRK is then created for each CRH bin, from which an individual cloud feedback for each CRH bin is computed. This allows for the spectrum of climate states in the RCE simulations with organized convection to be captured, similarly to how studies using GCMs consider different regional climates. This is different from what was created for RCE_small in Stauffer and Wing (2023), where only one histogram was created per model.

The discussion of the cloud feedback (and its decomposition) will primarily make use of a representative cloud feedback for the *entire* domain, properly accounting for the effects of the range of climates. This is analogous to a tropical average cloud feedback. The representative cloud feedback, $\hat{f}$, is the weighted average over all CRH bins, in which the cloud feedback is weighted by the fraction of the total domain that falls within a given CRH bin, as given by Equation 1:

$$\hat{f} = \sum_{x=1}^{10} f(x) * ncol(x) / \sum_{x=1}^{10} ncol(x), \quad (1)$$

where $f(x)$ is the cloud feedback for a CRH bin, x, and $ncol(x)$ is the number of grids falling in a CRH bin, x. The fraction of the domain falling within a CRH bin uses the cold simulation distribution, our "base climate state."

Before we continue, we wish to acknowledge that, in this paper, we are limiting the cloud feedback analysis to only the classic changes in cloud amount, cloud optical depth, and CTP in both the domain mean and individual climates defined by CRH. For the CRK method to be applied to our climate regimes, we are assuming the distribution in CRH does not change with warming SST (i.e., $\hat{f}$ is weighted by the CRH distribution using the cold simulation only). This is, of course, not a perfect assumption. As seen in Figure S1 in Supporting Information S1, some models have a distribution in CRH that shifts toward moister bins (e.g., Figures S1c, S1d, and S1i in Supporting Information S1). More consistently, there is a tightening of the distribution toward the moister bins where less of the domain falls into the drier bins for the warmer simulations. We tested the robustness of our results to weighting the cloud feedback using the 305 K simulation CRH distribution as well as the average CRH distribution between 295 and 305 K and found that, while there are subtle differences on the individual levels (such as cloud feedback magnitudes), the conclusions regarding the cloud feedback comparison across CRH bins (Section 3.5) as well as the relationship with I_{org} (Section 4) remain unchanged.

Figure 1 shows the RCE_large CRM model-mean 300 K ISCCP histogram for each CRH bin, the model-mean CRH-weighted mean 300 K ISCCP histogram, calculated as in Equation 1 but for the ISCCP histogram not the cloud feedback, the model-mean RCE_small 300 K ISCCP histogram from Stauffer and Wing (2023), and ISCCP histograms for the model-mean 300 K CAM-GCM-RCE simulations for three representative CRH bins as well as the CRH-weighted mean. This captures a diversity in cloud types and a progression from one type to another as CRH increases within the simulations (Figures 1a–1j). This would have otherwise been missed if only one histogram was used for the entire domain (Figure 1k). For the driest areas, the clouds are all high and optically

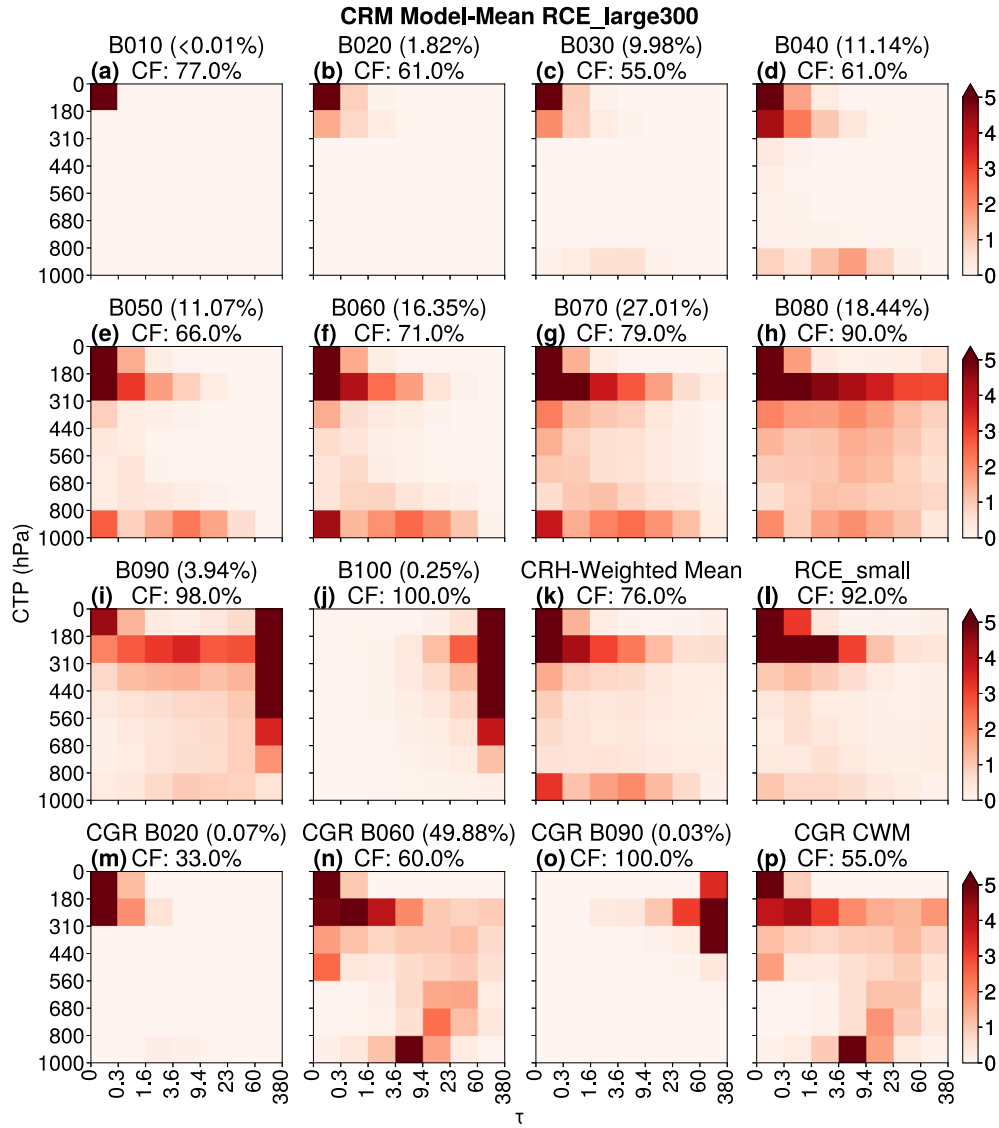

Figure 1. International Satellite Cloud Climatology Project histograms for the model-mean large domain 300 K (RCE_large300) cloud resolving models (CRMs) for each column relative humidity (CRH) bin (a–j) and the CRH-weighted mean (k), the small domain (RCE_small) model-mean (l) from Stauffer and Wing (2023), and the mean of CAM5-GCM-RCE and CAM6-GCM-RCE for three representative CRH bins (m–o) and the CRH-weighted mean (p). Shading shows the percentage of columns in that cloud top pressure (CTP)-τ bin. The top-most number for each panel is the percent of the domain with CRH contained within that bin and the bottom-most number for each panel is the total cloud amount for that histogram (the total sum of the histogram).

thin, which are possibly detached anvils (Figures 1a–1c). For the moister areas, there is a larger presence of low- and mid-level clouds and the high clouds are thicker (Figures 1d–1f). The mid-level clouds in the moistest part of the domain are optically thicker and there are less low clouds while the completely saturated regions only have a deep convective core as seen by the optically-thick clouds that span the full free troposphere (Figures 1g–1j). The majority of the columns in the domain are present in the B060, B070, and B080 CRH bins (50%–80% CRH, Figures 1f–1h), which is reflected in the CRH-weighted mean histogram (Figure 1k). This general description is for the CRM model-mean only, each model exhibits its own cloud distribution as a function of CRH where the bin with the greatest frequency of occurrence varies across models but still lies in the B060, B070, and B080 CRH bins (50%–80% CRH). The CRH-weighted mean favors the B050, B060, and B070 CRH bins (40%–70% CRH) *or* the B060, B070, and B080 CRH bins (50%–80% CRH) for the majority of the RCE_large CRMs. Figure S2 in

Supporting Information S1 shows the individual histograms for each model, binned in the manner shown in Figure 1 for the 300 K RCE simulations.

2.3. Cloud Feedback Decomposition

The CRK for each CRH bin in a model is found by computing top of atmosphere radiative fluxes using the Rapid Radiative Transfer Model-GCM (RRTMG, Iacono et al., 2008), a commonly used radiative transfer scheme, as interfaced by `climlab` (Rose, 2018; Stauffer & Wing, 2023; Zelinka et al., 2012a). This requires profiles of cloud liquid and ice water paths, temperature, trace gas profiles (Wing et al., 2018), surface emissivity, and albedo properties. Liquid effective radius is set to a constant 14 μm and the effective ice radii profile is defined as in Kiehl et al. (1998). RRTMG is run for the 64 different CTP-τ combinations in the ISCCP histogram in cloudy-sky mode, where the all-sky kernel has a single-layer cloud placed in the pressure layer given by a particular CTP and cloud water and cloud ice are prescribed by a given τ, as well as clear-sky mode, where cloud liquid and ice water are zeroed out everywhere. The radiative fluxes for the 49 ISCCP bins are found by averaging the corners of each CTP-τ bin and, when divided by 100%, returns the final CRK.

The cloud feedback uses the SST-mean and model-mean CRK, as well as the difference between a warm and cold ISCCP histogram to produce cloud-induced radiative flux anomalies following Equation B10 of Zelinka et al. (2013). This allows the cloud feedback to be decomposed into its components due to changes in cloud amount, CTP, and cloud optical depth individually. These decomposed cloud feedbacks are also separated into two altitude components: a non-low (free-troposphere) cloud component associated with CTP < 680 hPa, and a low (boundary layer) cloud component associated with CTP ≥ 680 hPa (Zelinka et al., 2016), which are referred to as HI680 and LO680, respectively, while the all sky cloud feedback is referred to as ALL. The cloud amount component (f_{amt}) describes the feedback due to changes in total cloud amount holding relative proportions of cloud amount in each CTP and τ bin constant, the cloud altitude component (f_{alt}) due to the changes in the vertical distribution of clouds holding total amount and optical depth distribution fixed, and the cloud optical depth component (f_{tau}) due to the anomalous optical depth distribution of clouds holding total amount and vertical distribution fixed.

2.4. Organization Metrics

In this paper, we are concerned with how the cloud feedback differs in models with various degrees of organization. To describe the degree to which a domain organizes we use a metric called the index of organization (I_{org}). I_{org} is a clustering metric that compares the nearest neighbor distribution of deep convective entities to that of a random distribution: values greater than 0.5 mean the convection is organized while the closer I_{org} gets to 1.0, the more organized the domain is (Tompkins & Semie, 2017). Specifically, we use the average I_{org} across the three SSTs ($\langle I_{org} \rangle$) as well as the change in I_{org} between the 295 and 305 K simulations (ΔI_{org}). I_{org} values were obtained from Wing et al. (2020a).

Due to the possibility that large and highly-influential outliers may skew the significance of otherwise highly correlated relationships, the studentized residual is used to filter outliers (Cook & Weisberg, 1982). The studentized residual is the leave-one-out prediction error at each observation and is used here to identify outliers. Specifically, a model is identified as an outlier if the absolute value of its studentized residual is greater than the Bonferroni corrected critical value, which is set to two to avoid over filtering the relatively small sample size of this data set. The correlation between the cloud feedbacks and the metrics are determined using the Pearson correlation coefficient with significance determined by a p-value of less than 0.05. Sometimes, one filter using the studentized residual still neglected to identify a potentially influential outlier, so a second pass was run on the remaining models, which improved correlations and significance without over-filtering the models. Any relationships discussed throughout Section 4 considers only the statistically significant correlations between the cloud feedbacks and $\langle I_{org} \rangle$ when the outlier filter described here is applied twice.

3. Cloud Feedbacks in RCE_Large

The first effect of convective self-aggregation we explore is whether the mere *existence* of organized convection affects cloud feedbacks. Here, we compare the cloud feedback and its components in RCE_large to those in RCE_small (Stauffer & Wing, 2023), where we use the CRH-weighted mean cloud feedback ($\hat{f}$, Equation 1) for RCE_large as it is the most comparable to that of RCE_small.

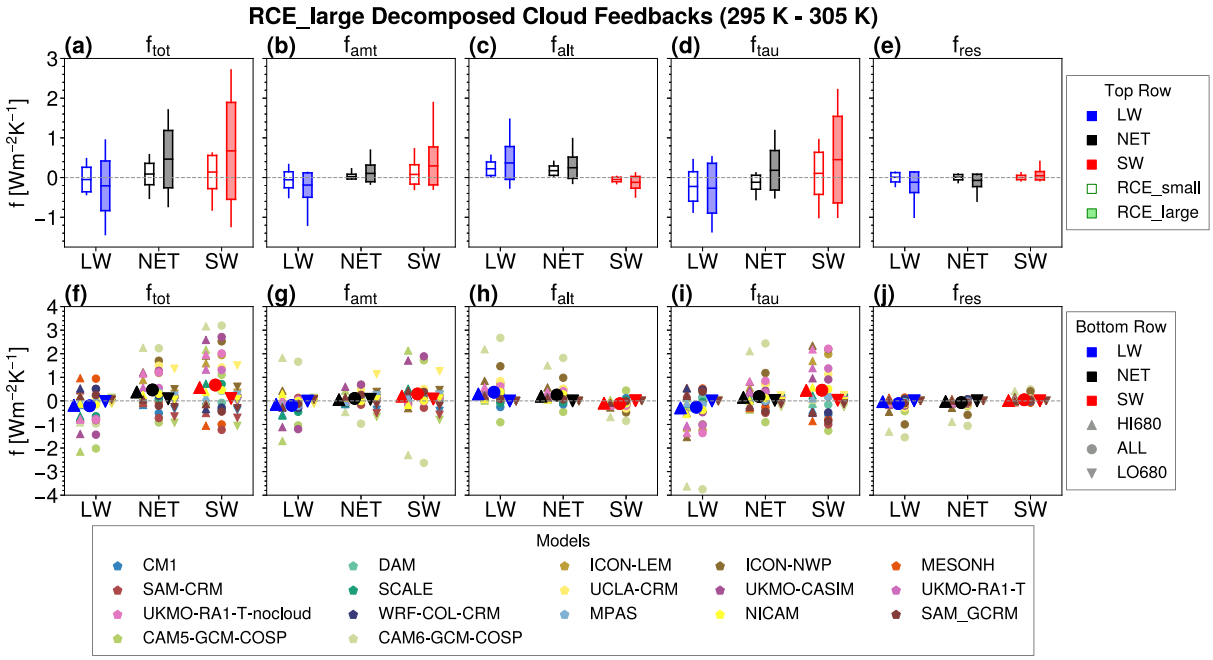

Figure 2. The cloud feedback decomposed into its contributions by cloud amount (b, g), cloud altitude (c, h), and cloud optical depth (d, i), as well as its residual (e, j) and the total cloud feedback (a, f) following Zelinka et al. (2013). The top row contains box and whisker plots (where the whiskers extend to the range of the data and the box is bound by plus and minus one standard deviation) for the small domain (RCE_small) ALL cloud feedbacks from Stauffer and Wing (2023) (left boxes, no shading) and the large domain (RCE_large) using $\hat{f}$ (right boxes, shaded). The bottom row contains the HI680 (upward triangles), ALL (circles), and LO680 (downward triangles) cloud feedbacks for RCE_large, using $\hat{f}$. Individual models are represented by the smaller shapes, with color varying depending on model. The larger shapes are the model-mean cloud feedback. In both the top and bottom row, blue is the longwave cloud feedback, black is the net cloud feedback, and red is the shortwave cloud feedback.

The model-mean cloud feedback and its components in RCE_large have a magnitude that is (on average) three times that found in RCE_small and shares the sign for all components except the net cloud optical depth feedback, which will be discussed further in Section 3.4 (Figure 2, Table 2). The majority of models in RCE_large have cloud feedbacks with larger magnitudes than RCE_small (six times as large, on average, when outliers are not considered). For all but 3 of the 12 models which have both a RCE_small and RCE_large simulation, the majority of the 36 cloud feedback components have the same sign (i.e., the existence of organized convection tends to not influence whether the cloud feedback dampens or amplifies the initial perturbation). These 36 cloud feedback components consist of the four decomposed components of the cloud feedback over the three altitude ranges (LO680, HI680, All) for each of longwave, shortwave, and net, Figures 2f–2j.

The larger magnitude cloud feedbacks in RCE_large are a consequence of low cloud feedbacks that do not occur in RCE_small. Unlike RCE_small, RCE_large produces a more diverse range of cloud types that includes low clouds (compare Figure 1k to Figure 1l; the low cloud portion of the histogram is isolated in Figure S3 in Supporting Information S1). Since properties of the low clouds in RCE_large change with warming, such as LO680 cloud amount, the contribution of the associated low cloud feedback increases the total cloud feedback. This is especially so in the CRH bins that encompass the range of CRH in RCE_small (B060, B070, and B080; see Figure S3 in Supporting Information S1). While RCE_small has a marginal increase in LO680 cloud amount, RCE_large has various combinations of increasing and decreasing LO680 cloud amount within the CTP-τ bins. Indeed, one of the more distinct differences between RCE_small and RCE_large is the larger LO680 cloud feedbacks in RCE_large relative to those in RCE_small (Figure S3 in Supporting Information S1). Where appropriate, we distinguish specific contributions by HI680 and LO680 for RCE_large below.

3.1. The Total Cloud Feedback

The net total cloud feedback for RCE_large is, on average, 0.46 ± 0.72 Wm^{-2} K^{-1} (Figures 2a and 2f, also Table 2), which is just over three times that found in RCE_small (0.14 ± 0.20 when a negative outlier was removed, Stauffer & Wing, 2023). There are four models in RCE_large with a negative total cloud feedback,

Table 2
Cloud Feedbacks (Wm^{-2} K^{-1}) Decomposed Into Its Contributions by Cloud Amount, Cloud Altitude, and Cloud Optical Depth, As Well As Its Residual and the Total Cloud Feedback Following Zelinka et al. (2013) for the RCE_Large Model-Mean

	HI680	ALL	LO680
Longwave cloud feedbacks			
tot	−0.19 ± 0.62	−0.21 ± 0.63	−0.02 ± 0.05
amt	−0.15 ± 0.38	−0.19 ± 0.31	−0.01 ± 0.05
alt	0.29 ± 0.21	0.37 ± 0.41	−0.01 ± 0.01
tau	−0.30 ± 0.66	−0.27 ± 0.63	0.00 ± 0.01
err	−0.03 ± 0.13	−0.12 ± 0.26	0.00 ± 0.00
Net cloud feedbacks			
tot	0.38 ± 0.48	0.46 ± 0.72	0.09 ± 0.43
amt	0.05 ± 0.17	0.10 ± 0.21	0.07 ± 0.36
alt	0.20 ± 0.14	0.25 ± 0.27	0.00 ± 0.00
tau	0.15 ± 0.35	0.18 ± 0.50	0.02 ± 0.09
err	−0.02 ± 0.08	−0.07 ± 0.16	0.00 ± 0.00
Shortwave cloud feedbacks			
tot	0.56 ± 1.03	0.67 ± 1.22	0.11 ± 0.48
amt	0.20 ± 0.46	0.29 ± 0.48	0.08 ± 0.41
alt	−0.10 ± 0.07	−0.12 ± 0.15	0.00 ± 0.00
tau	0.45 ± 1.00	0.45 ± 1.09	0.03 ± 0.10
err	0.01 ± 0.05	0.05 ± 0.10	0.00 ± 0.00

averaging -0.38 ± 0.30 Wm^{-2} K^{-1}, and 11 models with a positive total cloud feedback, averaging 0.77 ± 0.61 Wm^{-2} K^{-1}, both of which are larger than the RCE_small counterparts at -0.29 ± 0.21 and 0.22 ± 0.16, respectively (Stauffer & Wing, 2023).

3.2. The Cloud Altitude Feedback

The cloud altitude feedback is positive in the net (Figures 2c and 2h). This is expected due to the well understood response of cloud altitude to warming, in which rising cloud tops, holding all else fixed, would decrease the radiative cooling to space. Cloud tops rise with warming SST because convection is constrained by the Clausius-Clapeyron relationship to the pressure levels for which water vapor cools efficiently (Hartmann & Larson, 2002; Stauffer & Wing, 2022, 2023; Zelinka & Hartmann, 2010). The rising and slight warming of cloud tops, due to the more statically stable atmosphere, is observed in multiple numerical studies as well as in observations (Aerenson et al., 2022; Kuang & Hartmann, 2007; Stauffer & Wing, 2022; Wetherald & Manabe, 1988; Zelinka & Hartmann, 2011). Particularly in the longwave, this is the cloud feedback component with the smallest disagreement in the sign of the cloud feedback across the models, a response that is consistent with that found in RCE_small. There are two models in RCE_large, CM1 and SCALE, for which the longwave and shortwave cloud altitude feedback components have opposing signs to the model-mean (negative and positive, respectively). This is due to middle clouds (180 hPa ≤ CTP < 680 hPa) shifting *downwards* to cloud top pressures of CTP ≥ 680 hPa, instead of upwards, with warming SST.

3.3. The Cloud Amount Feedback

The model-mean net cloud amount feedback (Figures 2b and 2g) is near-zero but slightly positive, especially when the decently large outlier (UKMO-CASIM) is removed, due to the near-equal and opposite effects by the longwave and shortwave. While the sign of the model-mean net cloud amount feedback generally follows the sign of the shortwave cloud amount feedback, subtle differences occur on the individual model level. The net cloud amount feedback for RCE_small, on the other hand, has almost complete cancellation between the longwave and shortwave component. This is similar to the behavior of the HI680 net cloud amount feedback for RCE_large, which has greater cancellation than the ALL and LO680 cloud feedbacks (Figure 2g), emphasizing that the RCE_small simulations are primarily composed of non-low clouds. The magnitudes of the HI680 longwave and shortwave components are, on average, within 35% of one another. Conversely, the LO680 net cloud amount feedback follows the shortwave component, whose magnitudes are 80% higher than the longwave component.

These behaviors are consistent with a decrease in cloud amount in combination with near-zero net CRE of high clouds (Hartmann & Berry, 2017). The decrease in cloud amount, at least for high clouds in RCEMIP, has been largely described as a consequence of the stability iris effect (Bony et al., 2016; Stauffer & Wing, 2022) where less clear-sky radiatively-driven divergence, and therefore anvil spread, is required to balance radiative cooling in the more statically-stable environment associated with warming surface temperatures.

3.4. The Cloud Optical Depth Feedback

Finally, the cloud optical depth feedback (Figures 2d and 2i), like in RCE_small (Stauffer & Wing, 2023), has the largest magnitudes and inter-model spread among the cloud feedback components. The model-mean cloud optical depth feedback is positive in the net and shortwave, which is associated with cloud optical depth decreasing with warming SST. The opposite occurs for just under half of the models, where there is a larger decrease in thin clouds ($\tau < 3.6$) accompanied by a more moderate increase in thicker clouds; that is, the cloud optical depth *increases* with warming SST, rather than decreases.

Although the sign of the longwave and shortwave component is the same between RCE_small and RCE_large, the net cloud optical depth feedback is on average *negative*, instead of positive, for RCE_small. The shortwave

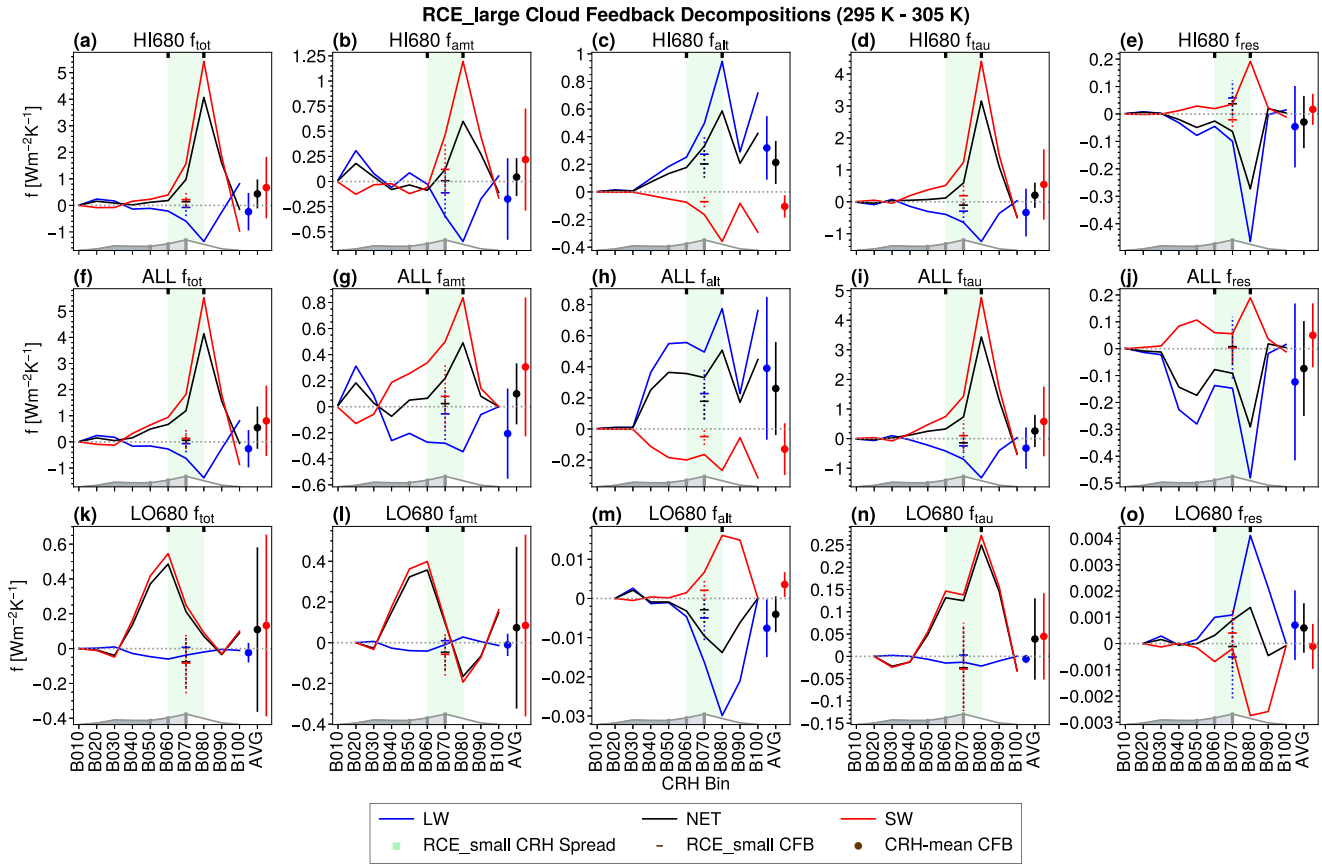

Figure 3. Model-mean decomposed cloud feedbacks for the longwave, net, and shortwave (blue, black, and red solid lines, respectively) as well as the model-mean $\hat{f}$ (three scatters at the right most part of the panels) with the spread across models denoted by the lines and defined as $\pm\sigma$. The top row is the HI680 cloud feedbacks, the middle row is the ALL cloud feedbacks, and the bottom row is the LO680 cloud feedbacks. The green shading between B060 and B090 is the spread in column relative humidity (CRH) values in the small domain simulations (RCE_small) with the model-mean cloud feedbacks and $\pm\sigma$ spread for RCE_small given by the scatter at B070. The gray line at the bottom of each panel is the same in each panel and represents the relative concentration of grid points (averaged across models) within a given CRH bin: from B010 to B050 represents 37% of the domain, from B050 to B060 16% of the domain, and from B060 to B070 27% of the domain, so that the total shading from B010 to B070 represents 80% of the domain.

effects of clouds (specifically HI680 clouds) in an organized domain plays a key role in this result with additional cascading effects that will be discussed further in Sections 4 and 5. This is especially so given the model-mean longwave cloud optical depth feedback is approximately equal between the two domains. The LO680 cloud optical depth feedback is negligible in RCE_large, limited by the lack of substantially thick clouds in RCE.

3.5. CRH-Dependent Cloud Feedback

When convection organizes there are two climate extremes that emerge: a dry-subsiding region and a moist-convecting region. To study the difference in the cloud feedbacks across the climate spectrum within RCE_large, we present the relationship between cloud feedbacks and CRH using the cloud feedback at each CRH bin as opposed to using the CRH-weighted mean cloud feedback ($\hat{f}$, Equation 1). This is analogous to analyzing the cloud feedbacks in the deep tropics separately from those in the subtropics.

Figure 3 plots the RCE_large model-mean cloud feedback for each cloud feedback component against the CRH bins (bin name definitions are given in Table 1). The model-mean and inter-model spread of $\hat{f}$ for RCE_large (Table 2) is the point on the right-most part of the figure. As described in Equation 1, the cloud feedbacks in each CRH bin shown in Figure 3 are weighted by their relative areas when averaging them to find $\hat{f}$. The point at B070 is the model-mean and inter-model spread of the RCE_small cloud feedbacks (Table S1 in Supporting Information S1, see also Stauffer & Wing, 2023), where the spread in CRH for RCE_small is contained within the B060 and B080 bins (50%–80% CRH), depicted by the green shading.

The model-mean cloud feedback (and its components) vary considerably across each individual CRH bin. There are three distinct features that emerge: (a) some individual CRH bins have cloud feedbacks that are greater than $\hat{f}$, (b) the cloud amount and cloud optical depth feedbacks go to zero as CRH approaches 0% *and* as CRH approaches 100%, and (c) the presence of low clouds in RCE_large introduces a cloud feedback component not present in RCE_small (the interpretation of LO680 in RCE_small is dubious, Stauffer & Wing, 2023). Figure S4 in Supporting Information S1 shows that, although the magnitudes of the cloud feedbacks are larger when using the CRH distribution for the 305 K simulation, these three patterns still occur. Over 80% of the domain has CRH $\leq$ 70% (the gray line and shading at the bottom of the panels in Figure 3). Since the cloud feedbacks tend to be smaller in the drier portions of the domain, which are weighted heavily when computing $\hat{f}$, $\hat{f}$ is much weaker than the extreme values found in moister bins. This is even more apparent when we look at the individual CRH cloud feedback components weighted by their relative area so that the total across all CRH bins is equivalent to $\hat{f}$ (Figure S5 in Supporting Information S1). Here, we see that the area-weighted cloud feedbacks for B070 (less than a third of the domain) makes up close to half or more of $\hat{f}$, and yet is still nowhere near the cloud feedback of a B070 region in isolation. We also note that, even when comparing the cloud feedbacks for RCE_large in the bins RCE_small are represented by (B060–B080), the cloud feedbacks in RCE_large generally have a larger magnitude than those in RCE_small. The changes in cloud amount are larger in RCE_large than RCE_small, especially for $\tau \geq 1.6$. As discussed toward the beginning of this section, RCE_large has more diverse cloud types, in both optical thickness and CTP. Because of the baseline different distribution of clouds in RCE_large, they are able to change even more and in different ways than in RCE_small. RCE_small clouds are primarily very high and thin and, as such, the primary change with warming SST is the decrease in cloud amount in this region. This doesn't necessarily imprint on the cloud feedback components that rely on changes in, for example, cloud optical depth. The cloud optical depth feedback component also contributes the most to the magnitude of the total cloud feedback in RCE_large for each individual CRH bin (compare the magnitudes of each component in Figure 3).

The second point, where the cloud feedback goes to zero for the driest and moistest parts of the domain, is explained by the distribution of cloud cover. While there are no (radiatively-relevant) clouds in the driest regions (CRH $\leq$ 10%, Figure 1a), there is 100% cloud cover in the moistest regions (CRH > 90%, Figure 1j), whose cloud properties are invariant with warming SST because it is characteristic of the deep convective core (i.e., troposphere-deep and optically thick clouds). If there are no changes in the optical thickness or amount of clouds in these areas with warming SST, there is no cloud feedback. We note that the cloud altitude component does not follow this pattern however, the focus of this is on the cloud optical depth feedback due to its considerable contribution to the total cloud feedback in both magnitude and its distribution across CRH bins.

Finally, the boundary layer cloud feedbacks in RCE_large are much smaller than those of the free troposphere where the LO680 cloud amount feedback is contributing the most to the LO680 total cloud feedback. Here, unlike all other components of the cloud feedback, there are two prominent extremes: a maximum at B060 and a minimum at B080 (where the single extreme occurs for the other cloud feedback components). However, the extreme at B080 is negligible for the LO680 total cloud feedback due to opposite contributions from the LO680 cloud amount feedback and LO680 cloud optical depth feedback. This is distinctly different from the total cloud feedback in HI680 and ALL.

3.6. Cloud Feedbacks in a Model With Parameterized Convection

The prior discussion regarding cloud feedbacks is the first of its nature for models with explicit convection configured in the RCE framework. Future work could compute the cloud feedback across models with different configurations in order to start to bridge the gap between RCE simulations and more comprehensive representations of Earth's climate. This could include comparing the results of this paper to those using CRM simulations configured similar to RCE_large but with SST gradients instead of constant SST, as is planned for the second phase of RCEMIP (Wing et al., 2023), or to those using aquaplanet GCM simulations with realistic rotation and SST gradients from CFMIP3 (Webb et al., 2017). Stauffer (2023a) performed a limited study with one CRM and one GCM of what effects SST gradients and rotation have on the cloud feedback compared to the RCE_large simulations. Here, we instead focus on expanding the discussion to a comparison of cloud feedbacks with one GCM configured in RCE, CAM-GCM-RCE, as an example of what could be done if all the GCM simulations in RCEMIP were re-run with the satellite simulator activated.

The CAM-GCM-RCE simulations have less cloud amount, but more types of clouds, than the RCE_large CRMs (Figures 1k and 1p). This is primarily because CAM-GCM-RCE has less HI680 clouds than RCE_large and less optically thin clouds ($\tau < 0.31$) than RCE_large (not shown). This gives credence to the conclusion that RCE CRM simulations over-produce high and thin clouds compared to models which parameterize convection (e.g., Stauffer & Wing, 2022; Wing et al., 2020a). Conversely, the CAM-GCM-RCE simulations have a greater amount of thick clouds, more than twice as many for $\tau \geq 23$, compared to RCE CRMs (not shown). To first order, this appears to be a consequence of the implementation of a convective parameterization scheme (Stauffer, 2023a). It should be noted that CAM6-GCM-RCE has been found to overproduce high, thick clouds at 305 K (Reed et al., 2021), but here only the 300 K simulation was considered.

Due to the spurious nature of CAM6-GCM-RCE at high SSTs (Reed et al., 2021) skewing the cloud feedback results, the remainder of this discussion will focus on CAM5-RCE-GCM as the feedback from 295 to 305 K. The use of a convection parameterization scheme does appear to have an impact on the cloud feedback in addition to the cloud distribution, compared to the RCE CRMs. Primarily, CAM-GCM-RCE has a larger cloud feedback magnitude than the RCE CRMs, regardless of whether or not CAM-GCM-RCE shares a sign with the RCE_large model-mean. The cloud feedbacks in CAM-GCM-RCE tend to fall near the edge or outside the range of the RCE_large CRMs (such as for the ALL longwave cloud amount feedback, Figure 2g). CAM-GCM-RCE also tends to be among the models that have an opposite sign from the RCE_large model mean such as seen for the cloud altitude or cloud optical depth feedbacks (Figures 2h and 2i). Finally, earlier in this section we found that the LO680 cloud feedbacks tend to be weaker than HI680 cloud feedbacks, a characteristic shared by the cloud feedbacks in CAM-GCM-RCE (Figure 2). Future work could extend this comparison between models with explicit convection and those with parameterized convection if other GCMs were run in RCE with the satellite simulator package enabled.

4. Influence of the Degree of Organization on the Cloud Feedback

4.1. Influence on the CRH-Weighted Mean Cloud Feedback

Having established that the mere *existence* of organized convection in a domain alters the cloud feedback, we now shift attention to studying how intermodel spread in the *degree* of organization influences cloud feedbacks. To do this, we look at the relationship across the RCE_large ensemble between $\hat{f}$ (the CRH-weighted mean cloud feedback) and $\langle I_{org} \rangle$ (the SST-averaged I_{org}). The correlation coefficients with outliers twice, once, and not filtered are given in Table S2 in Supporting Information S1. The third effect organized convection may have on cloud feedbacks concerns the *change* in aggregation with warming SST (ΔI_{org}). However, we found no concrete relationship between $\hat{f}$ and ΔI_{org} (Table S3 in Supporting Information S1). This was also found by Becker and Wing (2020). Although they found a correlation between climate sensitivity and the change in organization, the correlation was due to clear sky effects, not cloudy sky effects. However, we don't necessarily expect to find similar results because our method of calculating cloud feedbacks is much more comprehensive than that of Becker and Wing (2020), who simply examined the change in CRE with warming. That said, as discussed in Zelinka et al. (2013), the CRK method isn't completely different than other methods of computing cloud feedbacks, but it does allow us to describe the physical mechanisms in a more intuitive manner. Given ΔI_{org} having no apparent relation with the cloud feedbacks, the main text of this study focuses on the relationship between the cloud feedback and $\langle I_{org} \rangle$ while the discussion of ΔI_{org} is reserved for Text S1 and Table S3 in Supporting Information S1. The results using an alternate metric of organization are qualitatively similar but with a different statistical significance, see Text S2 and Tables S4 and S5 in Supporting Information S1.

We find that models with strongly organized convection have a negative net cloud feedback, while models with weakly organized convection have a positive cloud feedback (Figure 4e). This is primarily driven by the shortwave component, slightly offset by the longwave. The shortwave total cloud feedback (Figure 5e) is negative in strongly organized domains due to the negative HI680 shortwave cloud optical depth and the negative LO680 shortwave cloud amount feedbacks (Figures 5d and 5j). These shortwave cloud feedbacks have the opposite sign in weakly organized domains. The LO680 shortwave cloud altitude feedback is positive for the more strongly organized domains however, the magnitude of this component is several orders less than that of the negative shortwave cloud optical depth or cloud amount components (Figure 5k). On the other hand, the longwave total cloud feedback is positive for strongly organized domains and negative for weakly organized domains (Figure 6e) due to the contributions from the HI680 longwave cloud optical depth and LO680 longwave cloud amount

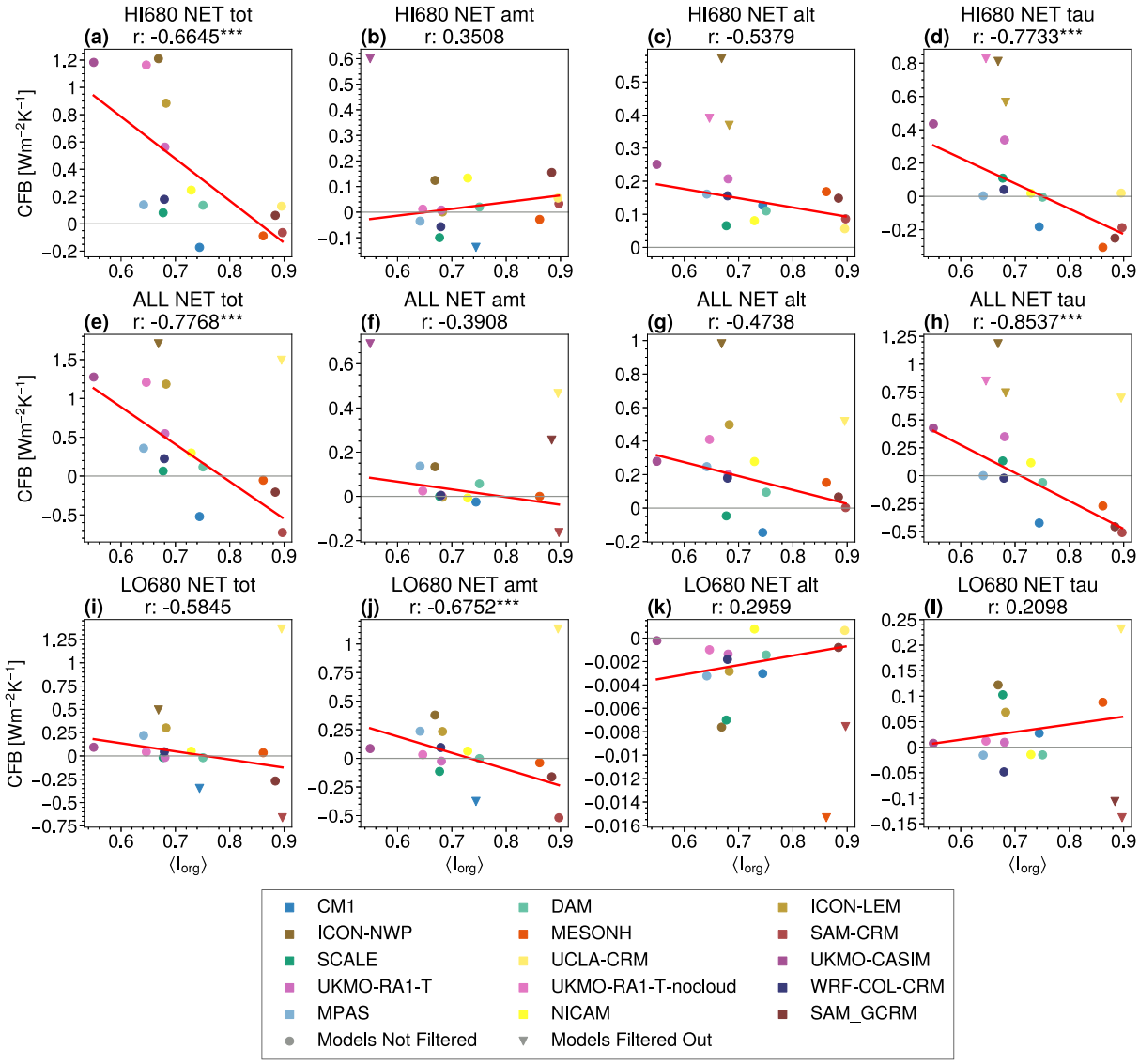

Figure 4. Decomposed net cloud feedback plotted against the index of organization (Wing et al., 2020a) averaged over all three sea surface temperature for the HI680 regime (a–d), the ALL regime (e–h), and the LO680 regime (i–l). The number at the top is the Pearson correlation coefficient, when outliers are twice filtered (red line), with significance at the 95% level denoted by the three stars.

components of the cloud feedback (Figures 6d and 6j). This only partially compensates the influence of organization on the shortwave feedback.

To determine what properties are driving these relationships, we will consider how the distribution of clouds within the ISCCP histogram changes with warming (ΔC) as well as the base state distribution of clouds within the ISCCP histogram itself (using 295 K, C_{295K}). In particular, the relationship and dependence of ΔC and C_{295K} on $\langle I_{org} \rangle$ and the cloud feedback component being considered is analyzed.

The cloud optical depth feedback relationship with $\langle I_{org} \rangle$, in which strongly organized domains have a less positive or negative shortwave cloud feedback and a less negative or positive longwave cloud feedback (Figures 5h and 6h), implies that the optical depth of the clouds is not reducing as much with warming SST for more organized domains, or it is even increasing with warming SST. Indeed, we found that the cloud distribution decreases for thinner clouds ($\tau < 0.3$) and, simultaneously, increases for thicker clouds ($0.3 \leq \tau < 0.36$) with warming SST (not shown), that is, the cloud optical depth is increasing with warming SST. This is especially so for HI680 clouds. When convection in a domain is more strongly organized, the HI680 clouds become thicker,

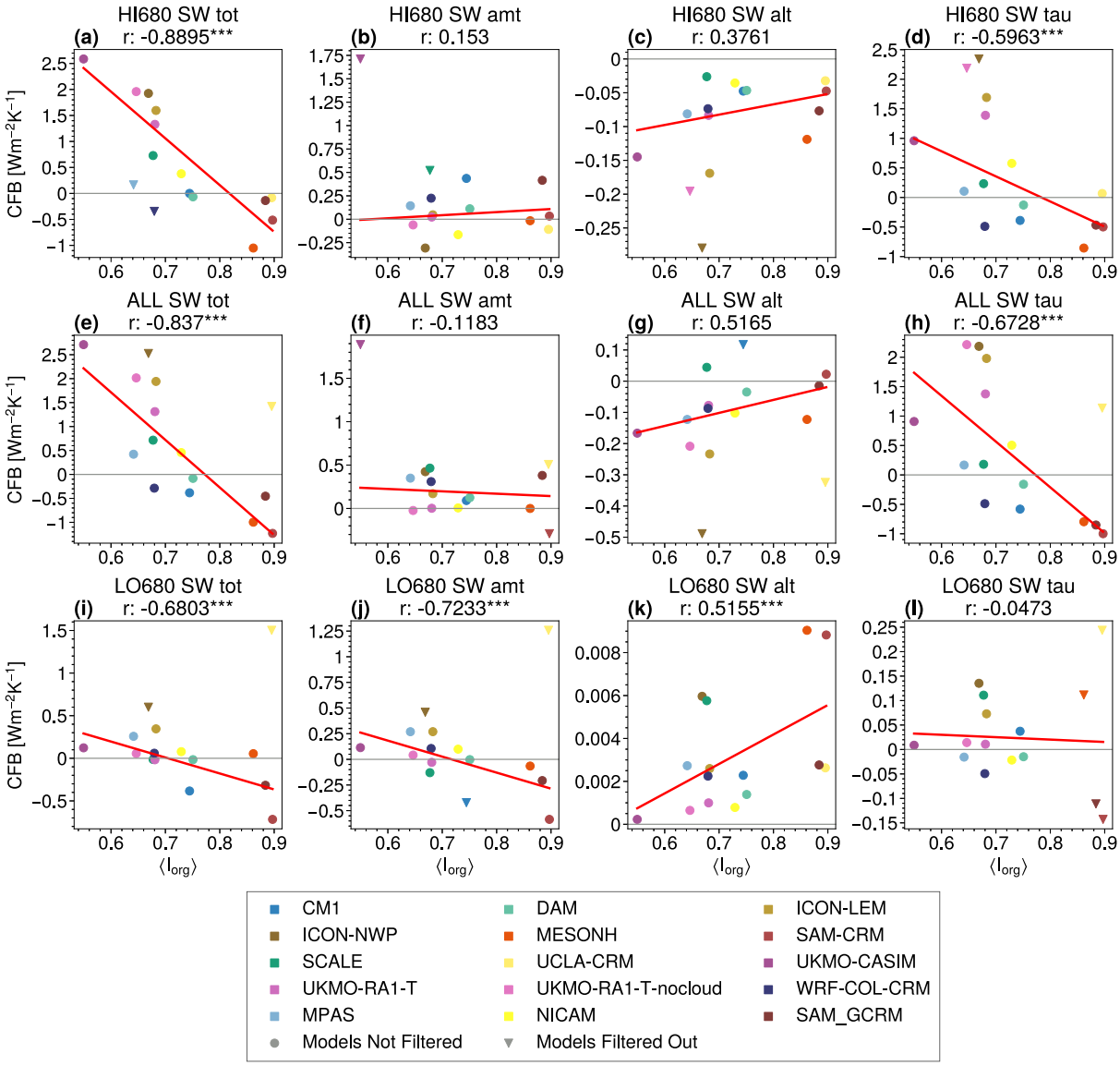

Figure 5. Decomposed shortwave cloud feedback plotted against the index of organization (Wing et al., 2020a) averaged over all three sea surface temperature for the HI680 regime (a–d), the ALL regime (e–h), and the LO680 regime (i–l). The number at the top is the Pearson correlation coefficient, when outliers are twice filtered (red line), with significance at the 95% level denoted by the three stars.

instead of thinner, with warming SST. Tobin et al. (2012, 2013) used satellite observations to analyze cloud properties of various states of organization in the tropics. They found that a more convectively organized state was associated with reduced cloudiness and a drier atmosphere. Here, we find that the decrease in high cloudiness is coming specifically from thinner optical depths so that the optical depth distribution is preferentially shifting toward higher optical thickness and, thereby, the subsequent increase in cloud optical thickness with warming in a more strongly organized environment. This then enhances the cooling effect in the shortwave and warming effect in the longwave.

The tendency for the positive shortwave total cloud feedback to be less positive or even negative, and the negative longwave total cloud feedback to be less negative or positive, for models that are more strongly organized also has a contribution from the LO680 cloud amount feedback (Figures 5j and 6j). This is predominantly due to the shortwave component because the LO680 longwave cloud feedbacks are generally small. Cloud tops that reside closer to the surface have emission temperatures similar to the surface and, therefore, a smaller longwave CRE. For LO680 clouds, cloud amount increases, as opposed to decreases, with warming SST for domains with

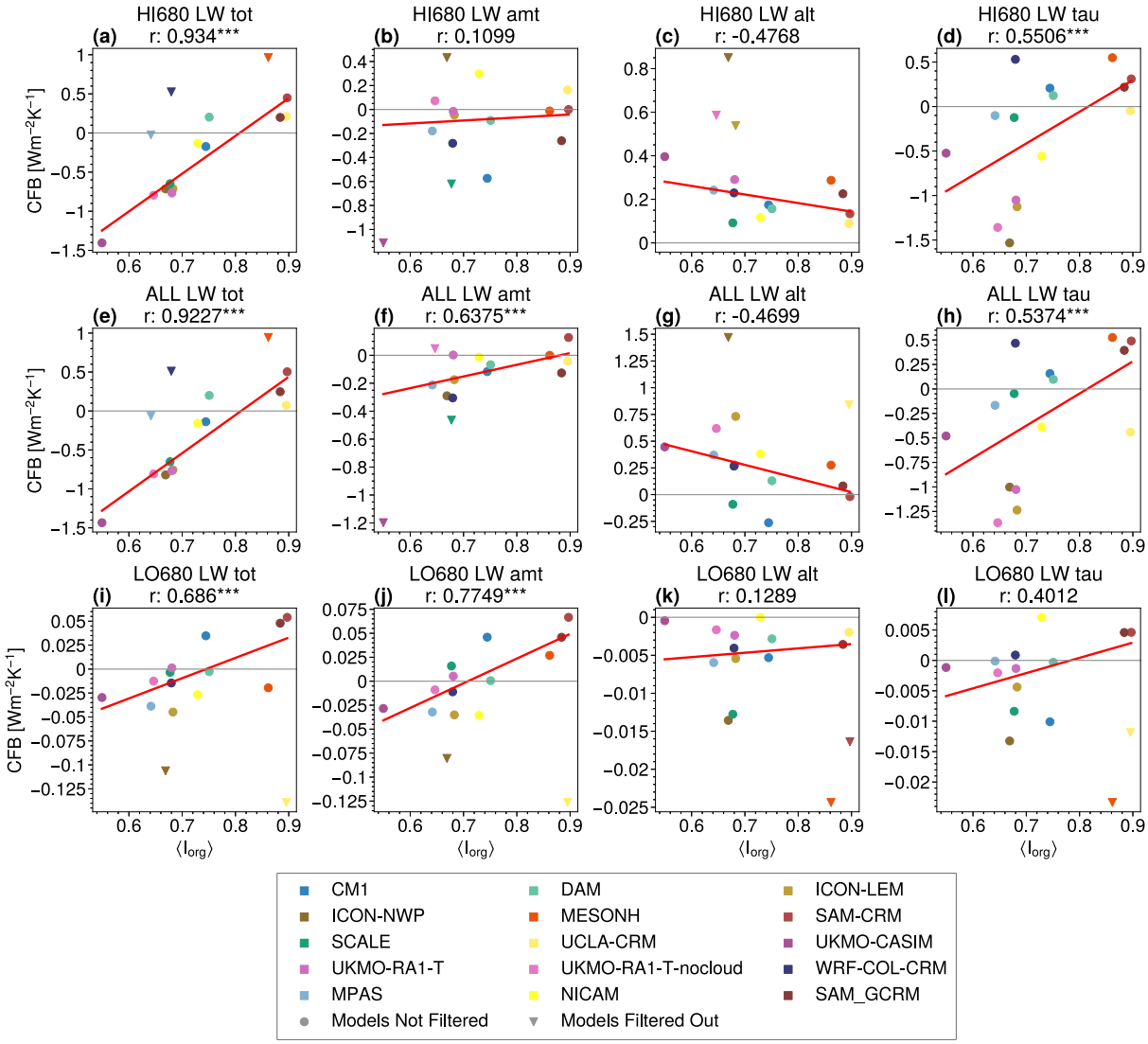

Figure 6. Decomposed longwave cloud feedback plotted against the index of organization (Wing et al., 2020a) averaged over all three sea surface temperature for the HI680 regime (a–d), the ALL regime (e–h), and the LO680 regime (i–l). The number at the top is the Pearson correlation coefficient, when outliers are twice filtered (red line), with significance at the 95% level denoted by the three stars.

stronger organization. This is especially so for clouds with $\tau \geq 1.6$. The LO680 cloud amount at 295 K is also higher for models with more strongly organized convection. Although the difference in the response of low-level cloud amount to warming SST with varying degrees of organization is not as well studied, there is consistently an increase in low-level cloudiness associated with the existence and greater degrees of organization in RCE (Cronin & Wing, 2017; Wing & Cronin, 2016; Wing et al., 2020a), which is different than the low-level cloudiness response to organization found in some observations (Tobin et al., 2012, 2013). While one of the primary benefits of RCEMIP is the inclusion of models that explicitly simulated convection, the kilometer-scale resolution still presents challenges in accurately representing low-level clouds.

Finally, the positive LO680 shortwave cloud altitude feedback is *more positive* for models with high degrees of organized convection (Figure 5k), associated with an increase in the cloud distribution for CTP ≥ 800 hPa with warming SST. However, its contribution to the total cloud feedback is negligible. The LO680 cloud amount at 295 K is also larger for larger values of $\langle I_{org} \rangle$, there are more boundary layer clouds to begin with for larger degrees of organization.

As discussed in Section 3.5, regardless of whether one uses the CRH distribution from the 295 K simulation, the 305 K simulation, or the average of the two, nearly all the correlations are the same sign and remain statistically significant (Table S6 in Supporting Information S1). There are a few, including the net total LO680 cloud feedback and the net HI680 cloud optical depth feedback, for which the correlation drops slightly below significance depending on which CRH distribution is used, due to slightly different compensation between the shortwave and longwave components. There is one correlation that changes sign, the one with the net LO680 cloud optical depth feedback, because a stronger negative correlation between I_{org} and the shortwave low cloud optical depth feedback emerges when the 305 K CRH distribution is used to calculate $\hat{f}$.

In summary, the net total cloud feedback is negative in models that are strongly organized and positive in those that are weakly organized. This is primarily driven by the impact of organization on the shortwave effect of HI680 cloud thickness. When the convection in a domain is more strongly organized, HI680 clouds get thicker with warming SST, instead of thinner as found in RCE_small and described for the model-mean. This causes the cloud optical depth feedback and, consequently, the total cloud feedback, to be negative.

4.2. Influence on the CRH-Dependent Cloud Feedback

As in Section 3.5, we consider the effects of the different CRH regimes on the relationship between the degree of organization and cloud feedbacks. For simplicity, we use four representative CRH regimes: "Very Dry" ($0\% < \text{CRH} \leq 20\%$), "Moderately Dry" ($20\% < \text{CRH} \leq 50\%$), "Moderately Moist" ($50\% < \text{CRH} \leq 80\%$), and "Very Moist" ($80\% < \text{CRH} \leq 100\%$). The correlations between $\langle I_{org} \rangle$ and the cloud feedbacks are shown in Figure 7, where significance at the 95% level are denoted by the shaded points.

The significant negative correlations between $\langle I_{org} \rangle$ and the net and shortwave total cloud feedbacks, and the significant positive correlation with the longwave total cloud feedback, as seen for $\hat{f}$, are found in all but the bins where $\text{CRH} \leq 20\%$. Like the case for $\hat{f}$, this is primarily driven by the relationship between $\langle I_{org} \rangle$ and the HI680 cloud optical depth feedback, contributed from bins where $\text{CRH} > 50\%$. It is not necessarily surprising that only the cloud feedbacks in the moist region are significantly correlated with the degree of organized convection within a simulation given that (a) cloud coverage relevant to cloud feedbacks is highest for $\text{CRH} > 50\%$ (Figure 1) and (b) only ∼1/3 of the domain is represented by $\text{CRH} \leq 50\%$, where over 43% of the domain is represented by $50\% < \text{CRH} \leq 80\%$, alone (Figure 3).

The negative correlation between $\langle I_{org} \rangle$ and the net and shortwave LO680 cloud amount feedback arises from the moderately dry regime, opposed by a positive correlation in the very moist regime. Similarly, the positive correlation between $\langle I_{org} \rangle$ and the longwave LO680 cloud amount feedback arises from the moderately dry to moderately moist bins, opposed by a negative correlation in the very moist bin. Thus, as found in Section 4.1, the relationship between the low-cloud feedback parameter and the degree of organization is largely associated with the drier parts of the domain. Finally, the positive correlation between $\langle I_{org} \rangle$ and the shortwave LO680 altitude feedback arises from the parts of the domain for which $\text{CRH} > 50\%$.

The CRH-dependent cloud feedbacks reveal a few relationships with $\langle I_{org} \rangle$ not seen for $\hat{f}$. In addition to the opposing behavior in the very moist bin for the LO680 cloud amount feedback, there are relationships between $\langle I_{org} \rangle$ and the HI680 cloud altitude feedback in the moderately to very moist bins. There is a positive correlation between $\langle I_{org} \rangle$ and the net and longwave HI680 cloud altitude feedback and a negative correlation with the shortwave HI680 cloud altitude feedback in the very moist bin. This is in contrast to the other bins and CRH-weighted mean, which have correlations of the opposite sign (significant only for the moderately moist bin). This suggests that, in the moistest part of the domain where, presumably, the strongest and deepest convective cores occur (e.g., as seen in Figure 1), the increase in cloud altitude with warming SST is enhanced in models with stronger organization.

The small differences notwithstanding, the relationship of $\hat{f}$ with $\langle I_{org} \rangle$ tends to follow the behavior of the moist bins ($\text{CRH} > 50\%$, which is just under two-thirds of the domain) but with magnitudes reduced by the weaker cloud feedbacks within the dry bins ($\text{CRH} \leq 50\%$, just over one-third of the domain).

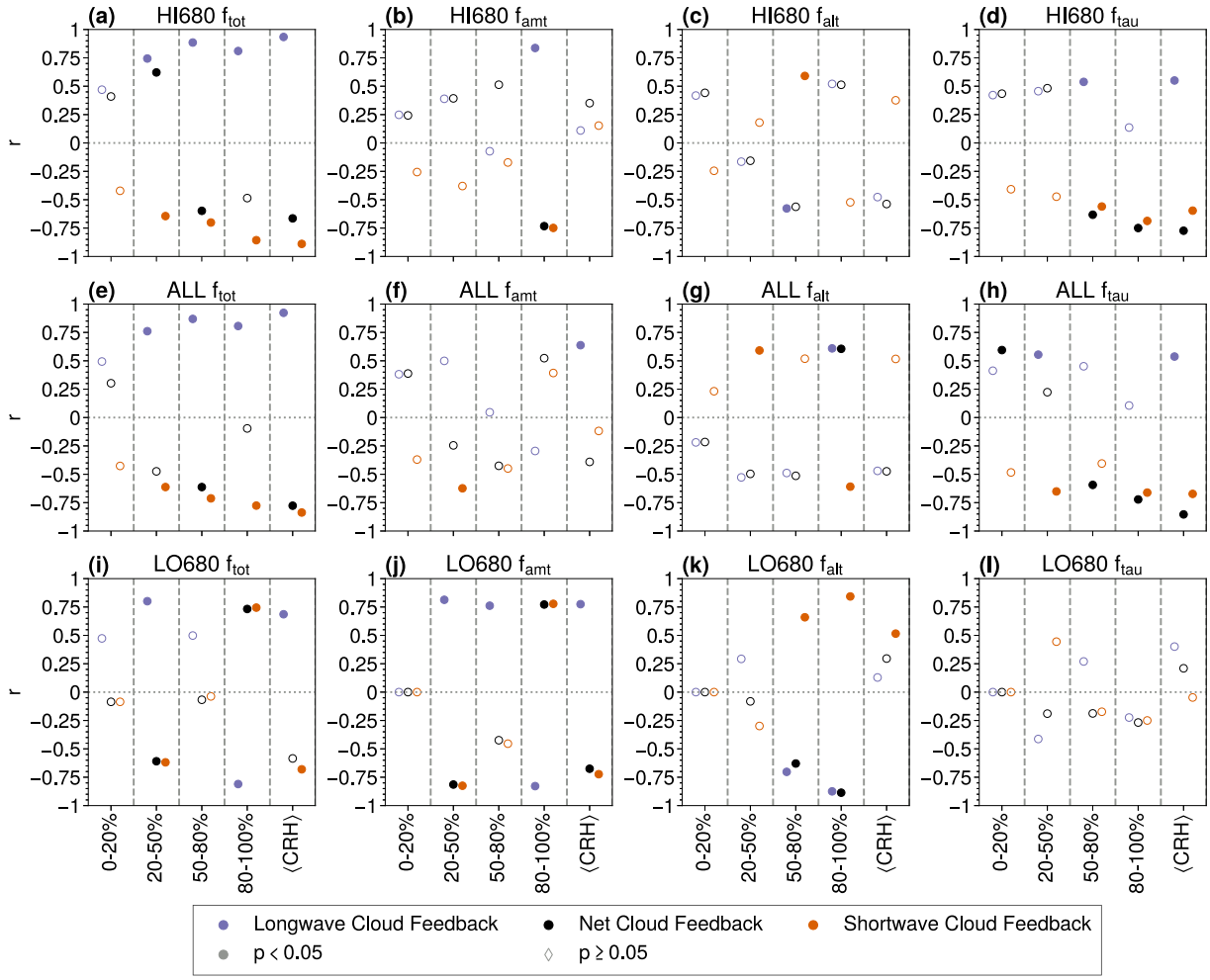

Figure 7. Correlations between the index of organization (Wing et al., 2020a), when the outliers are twice filtered, averaged over all three sea surface temperature and cloud feedbacks for the column relative humidity sub-regimes. Significance is determined at the 95% level and is displayed as the points with a solid shading. The blue points are the longwave cloud feedbacks, the black points are the net cloud feedbacks, and the orange points are the shortwave cloud feedbacks.

5. Comparison to an Expert Assessment

Finally, we compare the cloud feedback in RCE_large to those of phase five of the Coupled Model Intercomparison Project (CMIP5), CMIP6, and the expert assessment of Sherwood et al. (2020).

As discussed in Stauffer and Wing (2023), cloud feedbacks in RCE are most applicable to tropical-relevant assessed cloud feedbacks including the high-cloud altitude feedback, the tropical anvil cloud area feedback, and the tropical marine low-cloud feedback. While RCE_large simulations do have low clouds, the amount is still probably far less than reality and they lack substantial stratocumulus clouds. This is evident when comparing the RCE_large ISCCP histograms in Figure 1 to similar histograms derived from various satellite retrievals (e.g., Yue et al., 2016; Zhou et al., 2013).

The model-mean RCE_large high-cloud altitude feedback (Figures 8a and 8e), which was introduced in Section 3.2, is within the spread of prior work (the cloud feedbacks above the dashed line in Figure 8a), including RCE_small (the blue line in Figure 8a; Stauffer & Wing, 2023). The high-cloud altitude feedback is driven by the longwave response to an increase in cloud altitude with warming SST. CAM-GCM-RCE is on the low end of the inter-model spread while Stauffer (2023a) found that a CFMIP3 aquaplanet simulation (Webb et al., 2017), which is a simulation with parameterized convection but a more realistic configuration than RCE, agrees well with the RCE_large CRM and CMIP6 model-mean values.

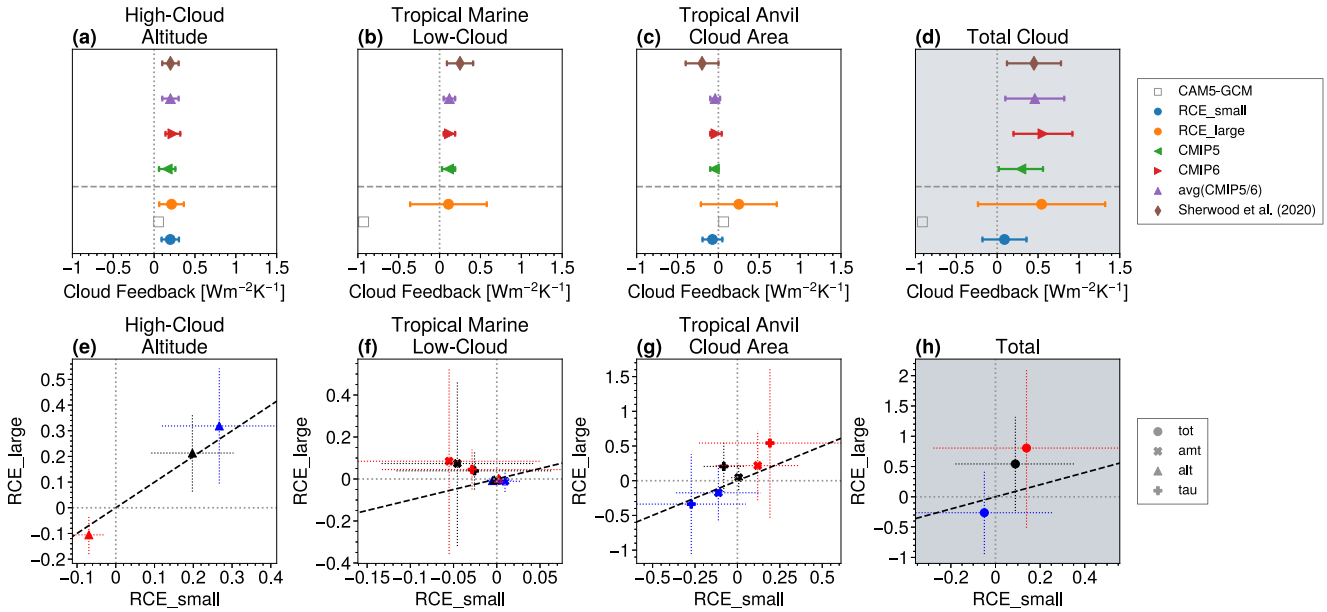

Figure 8. Top row: Radiative-convective equilibrium (RCE)-relevant decomposed cloud feedbacks for the RCE_small (Stauffer & Wing, 2023) and RCE_large simulations, the decomposed cloud feedbacks for the Coupled Model Intercomparison Project 5 (CMIP5), CMIP6, and the average of CMIP5 and CMIP6 (Zelinka et al., 2022), and the expert assessed cloud feedbacks (Sherwood et al., 2020). The scatter is the central value while the error bars demarcate $\pm\sigma$. The total cloud feedback is shaded gray to differentiate from the other cloud feedbacks because RCE does not include clouds such as land and arctic that are included in the CMIP and expert assessed values. Bottom row: the components that make up the cloud feedbacks in the top row (different symbols), the longwave component are the blue scatters, the net component the black scatters, and the shortwave component the red scatters.

The negative tropical anvil cloud area feedback anticipated from prior work (cloud feedbacks above the dashed line in Figure 8c; Sherwood et al., 2020) is not supported by the results of RCE_large (Figures 8c and 8g). Although there is a substantial amount of spread, the majority of the models are positive.

As defined by Sherwood et al. (2020) and Zelinka et al. (2022), the tropical anvil cloud area feedback is the sum of the HI680 cloud amount and cloud optical depth components. The cloud amount feedback is near-zero, contributing very little to the tropical anvil cloud area feedback due to cancellation between the shortwave and longwave components, which is consistent with recent observational constraints (McKim et al., 2023). As such, the positive result comes entirely from the positive cloud optical depth feedback. As presented in Section 3.4 (and Stauffer & Wing, 2023), positive shortwave cloud optical depth feedbacks and negative longwave cloud optical depth feedbacks occur due to HI680 clouds thinning with warming SST where, in RCE_large, the shortwave component governs the net cloud optical depth feedback. Figure 8g shows that the cloud optical depth and cloud amount feedbacks in both RCE_small and RCE_large consist of the same longwave and shortwave behavior, but the relative weight of the components differ between the domains. Except for the shortwave cloud optical depth feedback, whose magnitude in RCE_large is over twice the magnitude in RCE_small, the components for RCE_large are marginally lower than in RCE_small. Although the spread is considerable, this causes the shortwave component to be dominant for RCE_large, rather than the longwave component in RCE_small.

The tropical anvil cloud area feedback, consisting of both the HI680 cloud amount and HI680 cloud optical depth components, was identified as the most uncertain cloud feedback due to a lack of process understanding and known issues in GCM simulation of these cloud types (Sherwood et al., 2020). Prior best estimates of this feedback were moderately negative or near zero, reflecting the notion that either the longwave effects of a decrease in anvil cloud amount or a cancellation between shortwave and longwave effects would drive the feedback (Sherwood et al., 2020; Williams & Pierrehumbert, 2017). In RCE_large, the net HI680 cloud amount feedback is near zero, as suggested by prior work (Hartmann et al., 2001; Zelinka & Hartmann, 2011), but the HI680 cloud optical depth feedback is large and positive. As such, a positive cloud optical depth feedback cannot be ruled out as an essential component of the tropical anvil cloud response to warming.

Finally, the tropical marine low-cloud feedback (Figure 8b) has results that are more varied. The model-mean RCE_large cloud feedback is positive, like the previous studies, but the spread extends well into the negative where CAM-GCM-RCE lies. The largest contribution to this cloud feedback comes from the cloud optical depth and cloud amount feedback components, in particular, that in the shortwave (Figure 8f).

It cannot be understated how large the spread in the cloud feedbacks (as decomposed for comparison with Sherwood et al., 2020) is in the RCE_large simulations, especially for the tropical marine low-cloud and tropical anvil cloud area feedbacks. However, it isn't too surprising given the substantial spread in not only each of the cloud feedback components (Table 2) but also the spread in the degree of organization across the models (Wing et al., 2020a). The large spread could be explained by the different way in which clouds are distributed, the different strengths of the cloud feedbacks across the models, as well as the influence of the unconstrained nature of RCE simulations. The large spread also suggests that explicitly resolving convection does not immediately solve the problem of uncertainty in the cloud feedback. However, we expect that models with explicitly resolved convection are more accurately representing the processes underlying cloud feedbacks, and it is therefore important for us to know the full range of possible outcomes.

6. Conclusions

The cloud feedbacks (using $\hat{f}$) for the aggregated RCE_large simulations follow, for the most part, what was found for the unaggregated RCE_small simulations (Stauffer & Wing, 2023) but with larger magnitudes. That is, the existence of aggregation increases the magnitudes and the inter-model spread of the cloud feedbacks relative to simulations in which it is absent. However, this is a somewhat extreme comparison because we know that the real world does exhibit convective organization, as do climate models (at least to the extent resolved by their course grids). Climate models generally do not permit sub-grid scale convective organization, which means they could be missing a relevant process, however, even across simulations that all exhibit organization, the degree of organization may also influence cloud feedbacks. Indeed, across the RCEMIP ensemble, if a simulation is *more* organized than another simulation, the total net cloud feedback has a *smaller* value and is either less positive or less negative. This response follows the dependence of the total shortwave cloud feedback on the degree of aggregation; the total longwave cloud feedback is, instead, less negative or positive in more organized simulations.

The fact that the cloud feedbacks have a larger magnitude when convective organization exists (RCE_large) than when it doesn't (RCE_small) does not imply the same response to different degrees of organization within RCE_large. Instead, the cloud feedbacks in more strongly organized models have smaller values (or change sign) than those in weakly organized models. The relationship between cloud feedbacks and the degree of organization also does not imply a relationship between cloud feedbacks and changes in organization with warming (for which no relationship was found). The response of cloud feedbacks to the various properties of convective organization (its existence, degree, and change with warming) differs, which is somewhat counterintuitive. However, it isn't necessarily expected that these different properties of organized convection should affect the cloud feedbacks in the same way. Much like how the mechanisms governing the initiation of convective self-aggregation differ from those maintaining an organized state (Muller & Held, 2012; Wing et al., 2017), the mechanisms, characteristics, and impacts to the overall climate differ for these various properties of organization. Cronin and Wing (2017) argued how organization could affect climate feedbacks either through a change in organization with warming or through a more modest but likelier change in the impact of organization with warming, once organization is present (their Equation 7).

Here, we find that there are two separate changes in the cloud distribution with warming SST between the existence and variations in the degree of aggregation. We suggest that the existence of organized convection, and the varying climate and cloud regimes associated with it, offer new opportunities for clouds to change with warming. In RCE_small there is really only one type of cloud in the relatively spatially homogeneous domain. In RCE_large, on the other hand, there is a moisture-dependent distribution of clouds that includes a cloud regime that was barely present in RCE_small: low clouds. Changes in the amount of low clouds with warming in RCE_large allow for more varied and larger magnitude cloud feedbacks. The influence of the existence and degree of organization on the base state amount of low-level cloudiness is consistent. We find that the more organized a domain is, the higher the base state amount of low-level clouds and, at its most basic level, the

organized large domain simulations are technically more organized than the unorganized small domain simulations. Similar results are seen in prior modeling studies (Cronin & Wing, 2017; Wing & Cronin, 2016; Wing et al., 2017) and some observations (e.g., Stein et al., 2017) though not others (e.g., Tobin et al., 2012). However, what matters for cloud feedbacks is the change in cloud properties with warming, which can be more nuanced. While the organized domains have larger and more varied cloud feedbacks than the unorganized domains, primarily because the former have larger changes in low clouds with warming, the influence of the degree of organization on cloud feedbacks is mostly due to different changes in cloud optical depth with warming SST. Our results indicate that different representations of the degree of organization in the base state may contribute to intermodel spread in cloud feedbacks (though it, of course, is not the only potential source of such spread). Future work should attempt other ways of quantifying the relationship between cloud feedbacks and different levels of organization, such as a temporal evolution or dividing the domain into subdomains of more or less organization.

The shortwave cloud optical depth feedback plays an important role in not only the dependence of cloud feedbacks on organization but also in dictating the sign of the tropical anvil cloud area feedback. For RCE_large, the tropical anvil cloud area feedback is *positive*, which differs significantly from prior work and calls into question the expectation of a negative tropical anvil cloud area feedback due to the longwave effects of a decrease in cloud amount. Instead, the shortwave and longwave anvil cloud amount contributions largely cancel and a positive anvil cloud area feedback (consisting of the cloud amount and cloud optical depth components) results from the positive shortwave cloud optical depth contribution outweighing the negative longwave contribution. The shortwave cloud optical depth feedback also plays a secondary role in dictating the sign and magnitude of the tropical marine low-cloud feedback. Future work concentrated on understanding why cloud optical depth changes the way it does, and why it potentially changes *differently* in RCE CRM simulations, is potentially a good way forward in reducing uncertainty associated with tropical-relevant cloud feedbacks, especially those associated with tropical anvil clouds.

Finally, models that exhibit, in general, higher levels of organization would tend to have reduced climate sensitivity due to the associated smaller value cloud feedbacks. This is because now, instead of a positive cloud feedback associated with warming effects by clouds, the most organized domains have cooling effects associated with a negative cloud feedback. Understanding how convection organizes and how this is represented in models becomes paramount in accurately defining the role clouds will play in the surface temperature response to a changing climate.

Data Availability Statement

We thank the German Climate Computing Center (DKRZ) for hosting the standardized RCEMIP data (Wing et al., 2020b), which is publicly available at http://hdl.handle.net/21.14101/d4beee8e-6996-453e-bbd1-ff53b6874c0e. Data derived from the RCEMIP data set (Stauffer, 2023b) are archived at https://zenodo.org/records/10253539.

Acknowledgments
We acknowledge support by NSF AGS 1830724 and NSF AGS 2140419. We thank all co-authors on the RCEMIP overview paper (Wing et al., 2020a) for providing the RCEMIP simulations and Dr. Kevin Reed for providing the CAM-GCM-RCE simulations. We also thank Dr. Mark Zelinka for the cloud feedback decomposition software, Dr. Robert Pincus for discussions regarding ISCCP, and Dr. Brian Rose for the `climlab` software. We acknowledge high-performance computing support from Cheyenne at the NCAR-Wyoming Supercomputing Center (doi: 10.5065/D6RX99HX) provided by NCAR's Computational and Information Systems Laboratory, sponsored by the National Science Foundation. We would also like to thank four anonymous reviewers for their constructive and thorough reviews. CLS wishes to thank her Ph.D. committee members: Drs. Alyssa Atwood, Mark Bourassa, Eric Chicken, and Guosheng Liu for their support and early feedback on this work.

References

Aerenson, T., Marchand, R., Chepfer, H., & Medeiros, B. (2022). When will MISR detect rising high clouds? *Journal of Geophysical Research: Atmospheres*, *127*(2), e2021JD035865. https://doi.org/10.1029/2021JD035865

Becker, T., & Stevens, B. (2014). Climate and climate sensitivity to changing CO_2 on an idealized land planet. *Journal of Advances in Modeling Earth Systems*, *6*(4), 1205–1223. https://doi.org/10.1002/2014MS000369

Becker, T., Stevens, B., & Hohenegger, C. (2017). Imprint of the convective parameterization and sea-surface temperature on large-scale convective self-aggregation. *Journal of Advances in Modeling Earth Systems*, *9*(2), 1488–1505. https://doi.org/10.1002/2016MS000865

Becker, T., & Wing, A. A. (2020). Understanding the extreme spread in climate sensitivity within the radiative-convective equilibrium model intercomparison project. *Journal of Advances in Modeling Earth Systems*, *12*(10), e2020MS002165. https://doi.org/10.1029/2020MS002165

Bony, S., Semie, A., Kramer, R. J., Soden, B. J., Tompkins, A. M., & Emanuel, K. A. (2020). Observed modulation of the tropical radiation budget by deep convective organization and lower-tropospheric stability. *AGU Advances*, *1*(3), e2019AV000155. https://doi.org/10.1029/2019AV000155

Bony, S., Stevens, B., Coppin, D., Becker, T., Reed, K. A., Voigt, A., & Medeiros, B. (2016). Thermodynamic control of anvil cloud amount. *Proceedings of the National Academy of Sciences*, *113*(32), 8927–8932. https://doi.org/10.1073/pnas.1601472113

Bony, S., Stevens, B., Frierson, D. M. W., Jakob, C., Kageyama, M., Pincus, R., et al. (2015). Clouds, circulation and climate sensitivity. *Nature Geoscience*, *8*(4), 261–268. https://doi.org/10.1038/ngeo2398

Cess, R. D., & Potter, G. L. (1988). A methodology for understanding and intercomparing atmospheric climate feedback processes in general circulation models. *Journal of Geophysical Research*, *93*(D7), 8305–8314. https://doi.org/10.1029/jd093id07p08305

Cook, R. D., & Weisberg, S. (1982). *Residuals and influence in regression*. Chapman and Hall.

Coppin, D., & Bony, S. (2018). On the interplay between convective aggregation, surface temperature gradients, and climate sensitivity. *Journal of Advances in Modeling Earth Systems*, *10*(12), 3123–3138. https://doi.org/10.1029/2018MS001406

Cronin, T. W., & Wing, A. A. (2017). Clouds, circulation, and climate sensitivity in a radiative-convective equilibrium channel model. *Journal of Advances in Modeling Earth Systems*, *9*(8), 2883–2905. https://doi.org/10.1002/2017MS001111

Dufresne, J.-L., & Bony, S. (2008). An assessment of the primary sources of spread of global warming estimates from coupled atmosphere-ocean models. *Journal of Climate*, *21*(19), 5135–5144. https://doi.org/10.1175/2008JCLI2239.1

Fu, Q. (1996). An accurate parameterization of the solar radiative properties of cirrus clouds for climate models. *Journal of Climate*, *9*, 2058–2082. https://doi.org/10.1175/1520-0442(1996)009⟨2058:AAPOTS⟩2.0.CO;2

Hartmann, D. L., & Berry, S. E. (2017). The balanced radiative effect of tropical anvil clouds. *Journal of Geophysical Research: Atmospheres*, *122*(9), 5003–5020. https://doi.org/10.1002/2017JD026460

Hartmann, D. L., & Larson, K. (2002). An important constraint on tropical cloud-climate feedback. *Geophysical Research Letters*, *29*(20), 12-1–12-4. https://doi.org/10.1029/2002GL015835

Hartmann, D. L., Moy, L. A., & Fu, Q. (2001). Tropical convection and the energy balance at the top of the atmosphere. *Journal of Climate*, *14*(24), 4495–4511. https://doi.org/10.1175/1520-0442(2001)014⟨4495:TCATEB⟩2.0.CO;2

Held, I. M. (2005). The gap between simulation and understanding in climate modeling. *Bulletin of the American Meteorological Society*, *86*(11), 1609–1614. https://doi.org/10.1175/bams-86-11-1609

Hohenegger, C., & Stevens, B. (2016). Coupled radiative convective equilibrium simulations with explicit and parameterized convection. *Journal of Advances in Modeling Earth Systems*, *8*(3), 1468–1482. https://doi.org/10.1002/2016MS000666

Iacono, M. J., Delamere, J. S., Mlawer, E. J., Shephard, M. W., Clough, S. A., & Collins, W. D. (2008). Radiative forcing by long-lived greenhouse gases: Calculations with the AER radiative transfer models. *Journal of Geophysical Research*, *113*(D13), D13103. https://doi.org/10.1029/2008JD009944

Jakob, C., Singh, M. S., & Jungandreas, L. (2019). Radiative convective equilibrium and organized convection: An observational perspective. *Journal of Geophysical Research: Atmospheres*, *124*(10), 5418–5430. https://doi.org/10.1029/2018JD030092

Jeevanjee, N., Hassanzadeh, P., Hill, S., & Sheshadri, A. (2017). A perspective on climate model hierarchies. *Journal of Advances in Modeling Earth Systems*, *9*(4), 1760–1771. https://doi.org/10.1002/2017MS001038

Kiehl, J. T., Hack, J. J., Bonan, G. B., Boville, B. A., Williamson, D. L., & Rasch, P. J. (1998). The National Center for Atmospheric Research Community Climate Model: CCM3. *Journal of Climate*, *11*(6), 1131–1149. https://doi.org/10.1175/1520-0442(1998)011⟨1131:TNCFAR⟩2.0.CO;2

Klein, S. A., & Jakob, C. (1999). Validation and sensitivities of frontal clouds simulated by the ECMWF model. *Monthly Weather Review*, *127*(10), 2514–2531. https://doi.org/10.1175/1520-0493(1999)127⟨2514:VASOFC⟩2.0.CO;2

Knutti, R., Rugenstein, M. A. A., & Hegerl, G. C. (2017). Beyond equilibrium climate sensitivity. *Nature Geoscience*, *10*(10), 727–736. https://doi.org/10.1038/ngeo3017

Kuang, Z., & Hartmann, D. L. (2007). Testing the fixed anvil temperature hypothesis in a cloud-resolving model. *Journal of Climate*, *20*(10), 2051–2057. https://doi.org/10.1175/JCLI4124.1

Li, J.-L. F., Waliser, D. E., Chen, W.-T., Guan, B., Kubar, T., Stephens, G., et al. (2012). An observationally based evaluation of cloud ice water in CMIP3 and CMIP5 GCMs and contemporary reanalyses using contemporary satellite data. *Journal of Geophysical Research*, *117*(D16), D16105. https://doi.org/10.1029/2012JD017640

Maher, P., & Gerber, E. P. (2019). Atmospheric model hierarchies: Connecting theory and models. *Eos*, *100*. https://doi.org/10.1029/2019EO133929

Mauritsen, T., & Stevens, B. (2015). Missing iris effect as a possible cause of muted hydrological change and high climate sensitivity in models. *Nature Geoscience*, *8*(5), 346–351. https://doi.org/10.1038/ngeo2414

McKim, B., Bony, S., & Dufresne, J.-L. (2023). Physical and observational constraints on the anvil cloud feedback. *ESS Open Archive*. https://doi.org/10.22541/au.167769953.39966398/v2

Muller, C. J., & Held, I. M. (2012). Detailed investigation of the self-aggregation of convection in cloud resolving simulations. *Journal of the Atmospheric Sciences*, *69*(8), 2551–2565. https://doi.org/10.1175/JAS-D-11-0257.1

Ohno, T., Noda, A. T., & Satoh, M. (2020). Impacts of sub-grid ice cloud physics in a turbulence scheme on high clouds and their response to global warming. *Journal of the Meteorological Society of Japan. Series II*, *98*(5), 1069–1081. https://doi.org/10.2151/jmsj.2020-054

Ohno, T., Noda, A. T., Seiki, T., & Satoh, M. (2021). Importance of pressure changes in high cloud area feedback due to global warming. *Geophysical Research Letters*, *48*(18), e2021GL093646. https://doi.org/10.1029/2021GL093646

Ohno, T., & Satoh, M. (2018). Roles of cloud microphysics on cloud responses to sea surface temperatures in radiative-convective equilibrium experiments using a high-resolution global nonhydrostatic model. *Journal of Advances in Modeling Earth Systems*, *10*(8), 1970–1989. https://doi.org/10.1029/2018MS001386

Ohno, T., Satoh, M., & Noda, A. (2019). Fine vertical resolution radiative-convective equilibrium experiments: Roles of turbulent mixing on the high-cloud response to sea surface temperatures. *Journal of Advances in Modeling Earth Systems*, *11*(6), 1637–1654. https://doi.org/10.1029/2019MS001704

Reed, K. A., Silvers, L. G., Wing, A. A., Hu, I.-K., & Medeiros, B. (2021). Using radiative convective equilibrium to explore clouds and climate in the Community Atmosphere Model. *Journal of Advances in Modeling Earth Systems*, *3*(12), e2021MS002539. https://doi.org/10.1029/2021MS002539

Rose, B. E. J. (2018). CLIMLAB: A Python toolkit for interactive, process-oriented climate modeling. *Journal of Open Source Software*, *3*(24), 659. https://doi.org/10.21105/joss.00659

Rossow, W. B., & Schiffer, R. A. (1991). ISCCP cloud data products. *Bulletin of the American Meteorological Society*, *72*(1), 2–20. https://doi.org/10.1175/1520-0477(1991)072⟨0002:icdp⟩2.0.co;2

Sherwood, S. C., Bony, S., & Dufresne, J.-L. (2014). Spread in model climate sensitivity traced to atmospheric convective mixing. *Nature*, *505*(7481), 37–42. https://doi.org/10.1038/nature12829

Sherwood, S. C., Webb, M. J., Annan, J. D., Armour, K. C., Forster, P. M., Hargreaves, J. C., et al. (2020). An assessment of Earth's climate sensitivity using multiple lines of evidence. *Reviews of Geophysics*, *58*(4), e2019RG000678. https://doi.org/10.1029/2019RG000678

Slingo, A. (1989). A GCM parameterization for the shortwave radiative properties of water clouds. *Journal of the Atmospheric Sciences*, *46*(10), 1419–1427. https://doi.org/10.1175/1520-0469(1989)046⟨1419:AGPFTS⟩2.0.CO;2

Soden, B. J., & Held, I. M. (2006). An assessment of climate feedbacks in coupled ocean-atmosphere models. *Journal of Climate*, *19*(14), 3354–3360. https://doi.org/10.1175/JCLI3799.1

Soden, B. J., & Vecchi, G. A. (2011). The vertical distribution of cloud feedback in coupled ocean-atmosphere models. *Geophysical Research Letters*, *38*(12), L12704. https://doi.org/10.1029/2011GL047632

Stauffer, C. L. (2023a). Cloud feedbacks and convective self-aggregation in the radiative-convective equilibrium model intercomparison project (Order No. 30522899) (Doctoral dissertation). Florida State University, ProQuest Dissertations & Theses Global. Retrieved from https://www.proquest.com/dissertations-theses/cloud-feedbacks-convective-self-aggregation/docview/2868559250/se-2

Stauffer, C. L. (2023b). Cloud feedbacks and organized convection in radiative-convective equilibrium [Dataset]. *Zenodo*. https://doi.org/10.5281/zenodo.10253539

Stauffer, C. L., & Wing, A. A. (2022). Properties, changes, and controls of deep-convecting clouds in radiative-convective equilibrium. *Journal of Advances in Modeling Earth Systems*, *14*(6), e2021MS002917. https://doi.org/10.1029/2021MS002917

Stauffer, C. L., & Wing, A. A. (2023). Explicitly resolved cloud feedbacks in the radiative-convective equilibrium model intercomparison project. *Journal of Advances in Modeling Earth Systems*, *15*(11), e2023MS003738. https://doi.org/10.1029/2023MS003738

Stein, T. H. M., Holloway, C. E., Tobin, I., & Bony, S. (2017). Observed relationships between cloud vertical structure and convective aggregation over tropical ocean. *Journal of Climate*, *30*(6), 2187–2207. https://doi.org/10.1175/JCLI-D-16-0125.1

Swales, D. J., Pincus, R., & Bodas-Salcedo, A. (2018). The Cloud Feedback Model Intercomparison Project Observational simulator package: Version 2. *Geoscientific Model Development*, *11*(1), 77–81. https://doi.org/10.5194/gmd-11-77-2018

Tobin, I., Bony, S., Holloway, C. E., Grandpeix, J.-Y., Sèze, G., Coppin, D., et al. (2013). Does convective aggregation need to be represented in cumulus parameterizations? *Journal of Advances in Modeling Earth Systems*, *5*(4), 692–703. https://doi.org/10.1002/jame.20047

Tobin, I., Bony, S., & Roca, R. (2012). Observational evidence for relationships between the degree of aggregation of deep convection, water vapor, surface fluxes, and radiation. *Journal of Climate*, *25*(20), 6885–6904. https://doi.org/10.1175/JCLI-D-11-00258.1

Tompkins, A. M., & Craig, G. C. (1998). Radiative-convective equilibrium in a three-dimensional cloud-ensemble model. *Quarterly Journal of the Royal Meteorological Society*, *124*(550), 2073–2097. https://doi.org/10.1002/qj.49712455013

Tompkins, A. M., & Semie, A. G. (2017). Organization of tropical convection in low vertical wind shears: Role of updraft entrainment. *Journal of Advances in Modeling Earth Systems*, *9*(2), 1046–1068. https://doi.org/10.1002/2016MS000802

Vial, J., Dufresne, J.-L., & Bony, S. (2013). On the interpretation of inter-model spread in CMIP5 climate sensitivity estimates. *Climate Dynamics*, *41*(11–12), 3339–3362. https://doi.org/10.1007/s00382-013-1725-9

Waliser, D. E., Li, J.-L. F., Woods, C. P., Austin, R. T., Bacmeister, J., Chern, J., et al. (2009). Cloud ice: A climate model challenge with signs and expectations of progress. *Journal of Geophysical Research*, *114*(D8), D00A21. https://doi.org/10.1029/2008JD010015

Webb, M. J., Andrews, T., Bodas-Salcedo, A., Bony, S., Bretherton, C. S., Chadwick, R., et al. (2017). The cloud feedback model intercomparison project (CFMIP) contribution to CMIP6. *Geoscientific Model Development*, *10*(1), 359–384. https://doi.org/10.5194/gmd-10-359-2017

Webb, M. J., Senior, C., Bony, S., & Morcrette, J.-J. (2001). Combining ERBE and ISCCP data to assess clouds in the Hadley Centre, ECMWF and LMD atmospheric climate models. *Climate Dynamics*, *17*(12), 905–922. https://doi.org/10.1007/s003820100157

Wetherald, R. T., & Manabe, S. (1988). Cloud feedback processes in a general circulation model. *Journal of the Atmospheric Sciences*, *45*(8), 1397–1416. https://doi.org/10.1175/1520-0469(1988)045⟨1397:CFPIAG⟩2.0.CO;2

Williams, I. N., & Pierrehumbert, R. T. (2017). Observational evidence against strongly stabilizing tropical cloud feedbacks. *Geophysical Research Letters*, *44*(3), 1503–1510. https://doi.org/10.1002/2016GL072202

Wing, A. A. (2019). Self-aggregation of deep convection and its implications for climate. *Current Climate Change Reports*, *5*, 1–11. https://doi.org/10.1007/s40641-019-00120-3

Wing, A. A., & Cronin, T. W. (2016). Self-aggregation of convection in long channel geometry. *Quarterly Journal of the Royal Meteorological Society*, *142*(694), 1–15. https://doi.org/10.1002/qj.2628

Wing, A. A., Emanuel, K., Holloway, C. E., & Muller, C. (2017). Convective self-aggregation in numerical simulations: A review. *Surveys in Geophysics*, *38*(6), 1173–1197. https://doi.org/10.1007/s10712-017-9408-4

Wing, A. A., & Emanuel, K. A. (2014). Physical mechanisms controlling self-aggregation of convection in idealized numerical modeling simulations. *Journal of Advances in Modeling Earth Systems*, *6*(1), 59–74. https://doi.org/10.1002/2013MS000269

Wing, A. A., Reed, K. A., Satoh, M., Stevens, B., Bony, S., & Ohno, T. (2018). Radiative-convective equilibrium model intercomparison project. *Geoscientific Model Development*, *11*(2), 793–813. https://doi.org/10.5194/gmd-11-793-2018

Wing, A. A., Silvers, L. G., & Reed, K. A. (2023). RCEMIP-II: Mock-Walker simulations as Phase II of the radiative-convective equilibrium model intercomparison project. *Geoscientific Model Development Discussions*, *2023*, 1–38. https://doi.org/10.5194/gmd-2023-235

Wing, A. A., Stauffer, C. L., Becker, T., Reed, K. A., Ahn, M.-S., Arnold, N. P., et al. (2020a). Clouds and convective self-aggregation in a multimodel ensemble of radiative-convective equilibrium simulations. *Journal of Advances in Modeling Earth Systems*, *12*(9), e2020MS002138. https://doi.org/10.1029/2020MS002138

Wing, A. A., Stauffer, C. L., Becker, T., Reed, K. A., Ahn, M.-S., Arnold, N. P., et al. (2020b). Radiative-convective equilibrium model intercomparison project (RCEMIP) simulation dataset [Dataset]. *WDC Climate*. Retrieved from http://hdl.handle.net/21.14101/d4beee8e-6996-453e-bbd1-ff53b6874c0e

Yue, Q., Kahn, B. H., Fetzer, E. J., Schreier, M., Wong, S., Chen, X., & Huang, X. (2016). Observation-based longwave cloud radiative kernels derived from the a-train. *Journal of Climate*, *29*(6), 2023–2040. https://doi.org/10.1175/JCLI-D-15-0257.1

Zelinka, M. D., & Hartmann, D. L. (2010). Why is longwave cloud feedback positive? *Journal of Geophysical Research*, *115*(D16), D16117. https://doi.org/10.1029/2010JD013817

Zelinka, M. D., & Hartmann, D. L. (2011). The observed sensitivity of high clouds to mean surface temperature anomalies in the tropics. *Journal of Geophysical Research*, *116*(D23), D23103. https://doi.org/10.1029/2011JD016459

Zelinka, M. D., Klein, S. A., & Hartmann, D. L. (2012a). Computing and partitioning cloud feedbacks using cloud property histograms. Part I: Cloud radiative kernels. *Journal of Climate*, *25*(11), 3715–3735. https://doi.org/10.1175/JCLI-D-11-00248.1

Zelinka, M. D., Klein, S. A., & Hartmann, D. L. (2012b). Computing and partitioning cloud feedbacks using cloud property histograms. Part II: Attribution to changes in cloud amount, altitude, and optical depth. *Journal of Climate*, *25*(11), 3736–3754. https://doi.org/10.1175/JCLI-D-11-00249.1

Zelinka, M. D., Klein, S. A., Qin, Y., & Myers, T. A. (2022). Evaluating climate models' cloud feedbacks against expert judgment. *Journal of Geophysical Research: Atmospheres*, *127*(2), e2021JD035198. https://doi.org/10.1029/2021JD035198

Zelinka, M. D., Klein, S. A., Taylor, K. E., Andrews, T., Webb, M. J., Gregory, J. M., & Forster, P. M. (2013). Contributions of different cloud types to feedbacks and rapid adjustments in CMIP5. *Journal of Climate*, *26*(14), 5007–5027. https://doi.org/10.1175/JCLI-D-12-00555.1

Zelinka, M. D., Myers, T. A., McCoy, D. T., Po-Chedley, S., Caldwell, P. M., Ceppi, P., et al. (2020). Causes of higher climate sensitivity in CMIP6 models. *Geophysical Research Letters*, *47*(1), e2019GL085782. https://doi.org/10.1029/2019GL085782

Zelinka, M. D., Zhou, C., & Klein, S. A. (2016). Insights from a refined decomposition of cloud feedbacks. *Geophysical Research Letters*, *43*(17), 9259–9269. https://doi.org/10.1002/2016GL069917

Zhou, C., Zelinka, M. D., Dessler, A. E., & Yang, P. (2013). An analysis of the short-term cloud feedback using MODIS data. *Journal of Climate*, *26*(13), 4803–4815. https://doi.org/10.1175/JCLI-D-12-00547.1